Structural and Electronic Effects of Pentafluorophenyl Substituents on Cyclopentadienyl Complexes of Fe, Co, Mn, and Re[1]

Matthew P. Thornberry, Carla Slebodnick, and Paul A. Deck*

Department of Chemistry, Virginia Tech, Blacksburg, Virginia 24061-0212

Frank R. Fronczek

Department of Chemistry, Louisiana State University, Baton Rouge, Louisiana 70803-1804

Received September 18, 2000

The reaction of CpNa (Cp = C_5H_5) with C_6F_6 (diglyme, 110 °C, 14 h) afforded a mixture of products, from which two new triarylated cyclopentadienes, 1,2,4-$Ar_3C_5H_3$ (**3**) and 1,2,3-$Ar_3C_5H_3$ (**4**), were separated by silica gel chromatography (Ar = C_6F_5). The dienes **3** and **4** were readily converted (NaH, THF) to the corresponding triarylated sodium cyclopentadienides, (1,2,4-$Ar_3C_5H_2$)Na (**7**) and (1,2,3-$Ar_3C_5H_2$)Na (**8**). Reactions of the ligands **7** and **8** with $FeBr_2$ afforded the ferrocenes (1,2,4-$Ar_3C_5H_2)_2Fe$ (**11**) and (1,2,3-$Ar_3C_5H_2)_2Fe$ (**12**), respectively. The cobaltocenes $(ArC_5H_4)_2Co$ (**13**), (1,3-$Ar_2C_5H_3)_2Co$ (**14**), (1,2,4-$Ar_3C_5H_2)_2Co$ (**15**), and (1,2,3-$Ar_3C_5H_2)_2Co$ (**16**) were prepared from $CoBr_2$ and $(ArC_5H_4)Na$ (**5**), (1,3-$Ar_2C_5H_3$)Na (**6**), **7**, and **8**, respectively. Oxidation of **13** (air, dilute aqueous HCl) followed by precipitation with KPF_6 afforded $[(ArC_5H_4)_2Co]^+PF_6^-$ (**17**). The homologous cobaltocenium ions [1,3-$Ar_2C_5H_3]_2Co^+$ (**18**), (1,2,4- $Ar_3C_5H_2)_2Co^+$ (**19**), and (1,2,3-$Ar_3C_5H_2)_2Co^+$ (**20**) were observed (NMR) only after dissolving the corresponding Co^{II} species **14**−**16** in D_2SO_4; efforts to isolate **18**−**20** as hexafluorophosphates failed. Reactions of the ligands **5**−**8** with $M(CO)_5Br$ (M = Mn, Re) afforded the piano stool complexes (ArCp)$Mn(CO)_3$ (**21**), (1,3-Ar_2Cp)$Mn(CO)_3$ (**22**), (1,2,4-$Ar_3C_5H_2$)$M(CO)_3$ (**23**, M = Mn; **27**, M = Re), and (1,2,3-$Ar_3C_5H_2$)$M(CO)_3$ (**24**, M = Mn; **28**, M = Re). Both the voltammetric oxidation potentials ($E_{1/2}$) of the substituted metallocenes **9**−**16** and the carbonyl stretching wavenumbers of the substituted piano stool complexes **21**−**24** and **25**−**28** increased linearly with increasing number of C_6F_5 substituents. Crystal structures were obtained for **2** (two polymorphs), **4**, **11**, **16**, **23**, **26**, and **27**. Noteworthy features of these structures include C_6F_5−C_6F_5 arene stacking, C_6F_5 stacking with benzene solvate molecules, C_6F_5···O≡C−M interactions, and extensive C−H···F−C interactions. Barriers toward Cp−C_6F_5 rotation and Cp−Fe−Cp rotation were quantified for several of the complexes using dynamic ^{19}F and ^1H NMR spectroscopy.

Introduction

Cyclopentadienyl (Cp) complexes (e.g., **A**, **B**, and **C**) are known for nearly all metals, including several main group metals[2] and f-elements.[3] Ancillary ligand substituents (R) influence their molecular structures, physical properties,[4] and electrochemical and spectroscopic features.[5] Substituents also modulate the reactivity of other ligands (L, X) and bonds (M−L, M−X) in the inner coordination sphere,[6] which is particularly significant for catalysis.[7,8] While the size and shape (steric effects) of Cp substituents can control the orientation of substrate molecules approaching the metal, thereby optimizing regio- and stereoselectivity, electronic effects influence the degree to which a ligated metal atom can present orbitals having appropriate energy and spatial distribution to interact productively with organic substrates.[9]

Nevertheless, the study of electronic effects has lagged behind the study of steric effects.[10] One reason is the

(1) Parts of this work have been communicated orally: (a) Deck, P. A.; Thornberry, M. P. Southeast Regional Meeting of the American Chemical Society, Knoxville TN, October 17−20, 1999, Abstract 314. (b) Deck, P. A.; Thornberry, M. P. 215th National Meeting of the American Chemical Society, Dallas, TX, March 29−April 2, 1998, Abstract INOR 73. (c) Deck, P. A.; Thornberry, M. P. 218th National Meeting of the American Chemical Society, New Orleans, LA, August 22−26, 1999, Abstract INOR 525.

(2) (a) Overby, J. S.; Hanusa, T. P.; Boyle, P. D. *Angew. Chem., Int. Ed. Engl.* **1997**, *36*, 2378. (b) Burkey, D. J.; Hanusa, T. P. *J. Organomet. Chem.* **1996**, *512*, 165. (c) Overby, J. S.; Hanusa, T. P. *Organometallics* **1996**, *15*, 2205. (d) Burkey, D. J.; Hanusa, T. P. *Commun. Inorg. Chem.* **1995**, *17*, 41. (e) Jutzi, P.; Burford, N. *Chem. Rev.* **1999**, *99*, 969. (f) Harder, S. *Coord. Chem. Rev.* **1998**, *176*, 17. (g) Bridgeman, A. J. *J. Chem. Soc., Dalton Trans.* **1997**, *17*, 2887. (h) Sitzmann, H.; Dezember, T.; Ruck, M. *Angew. Chem., Int. Ed.* **1998**, *37*, 3114.

(3) (a) Evans, W. J.; Nyce, G. W.; Clark, R. D.; Doedens, R. J.; Ziller, J. W. *Angew. Chem., Int. Ed.* **1999**, *38*, 1801. (b) Arredondo, V. M.; McDonald, F. E.; Marks, T. J. *Organometallics* **1999**, *18*, 1949. (c) Klooster, W. T.; Brammer, L.; Schaverien, C. J.; Budzelaar, P. H. M. *J. Am. Chem. Soc.* **1999**, *121*, 1381. (d) Gunko, Y. K.; Edelmann, F. T. *Comm. Inorg. Chem.* **1997**, *19*, 153. (e) Molander, G. A.; Corrette, C. P. *J. Org. Chem.* **1999**, *64*, 9697.

(4) (a) Overby, J. S.; Hanusa, T. P.; Sellers, S. P.; Yee, G. T. *Organometallics* **1999**, *18*, 3561. (b) Hays, M. L.; Burkey, D. J.; Overby, J. S.; Hanusa, T. P.; Sellers, S. P.; Yee, G. T.; Young, V. G. *Organometallics* **1998**, *17*, 5521.

10.1021/om000798v CCC: $19.00
Publication on Web 11/14/2000

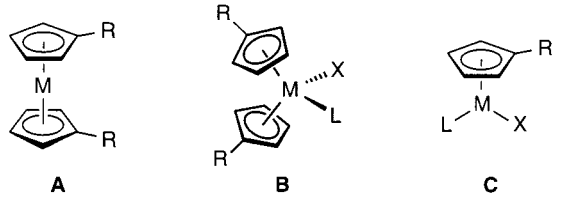

synthetic investment required to obtain a homologous series of complexes in which electronic effects vary widely.[11] Highly reactive substituents can require existing synthetic routes to be redesigned. For this reason, expected behavior of Cp complexes at the electron-donating or electron-withdrawing extremes is often inferred from trends observed over a narrow range of weakly electron-donating substituents such as CH_3 or $SiMe_3$, which are easy to attach and are usually inert toward the reagents and reaction conditions necessary for synthesis and catalytic screening.[12]

Our goal is to probe the electron-withdrawing extreme of substituent effects in Cp complexes using perfluoroaryl substituents. We showed earlier that one or two pentafluorophenyl (C_6F_5) groups are readily attached to cyclopentadiene and indene by nucleophilic aromatic substitution.[13,14] Unlike their perfluoroalkyl-substituted congeners,[15] C_6F_5-substituted Cp anions are stable as sodium salts, and they can be used in standard syntheses of various complexes of both early and late transition metals.[16] Although the fluoro (−F) substituent is also stable and highly electron-withdrawing, the synthesis of ring-fluorinated metallocene complexes has not yet been generalized beyond a few systems.[17] After our report, Hughes and co-workers showed that C_6F_5 groups are useful "crystal engineering" design elements,[16] while Rausch and co-workers showed that C_6F_5 substituents have significant effects on the polymerization of olefins by titanium Cp complexes.[18] Complementary studies at the electron-donating extreme have also appeared.[19]

This contribution reports the electron-withdrawing substituent effects that we have observed in several complexes bearing one to three C_6F_5 substituents attached to Cp ligands. First, we describe the syntheses of two regioisomeric tris(pentafluorophenyl)cyclopentadienes, which extend the series of mono- and bis(pentafluorophenyl)cyclopentadienes we reported earlier.[13] Then, we show how Cp ligands with 1−3 C_6F_5 groups can be used as ligands for Fe, Co, Mn, and Re. Electrochemical and spectroscopic data are presented to quantify the electronic substituent effects in these complexes. "Proof of concept" experiments using cobaltocene illustrate the potential of C_6F_5 substituents to stabilize 19-electron organometallic complexes. We then present the results of crystallographic studies that demonstrate the influence of C_6F_5 groups on molecular structure and crystal packing. Finally, we show how C_6F_5 groups affect static and dynamic aspects of metallocene conformations.

Experimental Section

General Procedures. Standard inert-atmosphere techniques were used for all reactions. C_6F_6 (99% purity) was received as a gift from Albemarle Corporation and used without further purification. $FeBr_2$, $Mn(CO)_5Br$, and $Re(CO)_5Br$ were used as received from Aldrich. NaH was purchased as a 60% mineral oil dispersion from Aldrich, washed with hexanes, dried under vacuum, and stored in a glovebox. Anhydrous $CoBr_2$ was prepared by heating the red commercial hydrate (Fisher) under vacuum to obtain a bright green powder. NaCp was prepared from freshly distilled cyclopentadiene and excess NaH in THF. Two ligands, **5** and **6**, were prepared as previously reported.[13] NMR experiments used JEOL Eclipse (500), Varian Unity (400), and Bruker EM (360) instruments. THF-d_8 was vacuum-transferred from Na/K alloy. ^{19}F NMR spectra were referenced to external C_6F_6 in $CDCl_3$ at −163.00 ppm. $\{^{19}F\}^{13}C$ NMR spectra were particularly useful for resolving signals in the aromatic C−F regions, particularly where extensive ^{19}F couplings in the ^1H-decoupled spectra prevented us from distinguishing closely spaced signals. C−F coupling constants were approximated from apparent splittings. Some of the complexes were insufficiently soluble for ^{13}C NMR analysis. Infrared spectra were recorded on a Midac M-series instrument operating at 1 cm^{-1} resolution. Mass spectra were obtained using a Fisons VG7070 instrument. Elemental analyses were performed by Desert Analytics (Tucson, AZ).

(5) (a) Blais, M. S.; Rausch, M. D. *Organometallics* **1994**, *13*, 3557. (b) Graham, P. B.; Rausch, M. D.; Taschler, K.; Von Philipsborn, W. *Organometallics* **1991**, *10*, 3049. (c) Meier, E. J. M.; Kozminski. W.; Linden, A.; Lustenberger, P.; von Philipsborn, W. *Organometallics* **1996**, *15*, 2469. (d) von Philipsborn, W. *Chem. Soc. Rev.* **1999**, *28*, 95. (e) Langmaier, J.; Samec, Z.; Varga, V.; Horacek, M.; Choukroun, R.; Mach, K. *J. Organomet. Chem.* **1999**, *584*, 323. (f) Barthel-Rosa, L. P.; Sowa, J. R.; Gassman, P. G.; Fischer, J.; McCarty, B. M.; Goldsmith, S. L.; Gibson, M. T.; Nelson, J. H. *Organometallics* **1997**, *16*, 1595. (g) Gassman, P. G.; Sowa, J. R.; Hill, M. G.; Mann, K. R. *Organometallics* **1995**, *14*, 4879. (h) Gassman, P. G.; Deck, P. A.; Winter, C. H.; Dobbs, D. A.; Cao, D. H. *Organometallics* **1992**, *11*, 959. (i) Bühl, M. *Organometallics* **1997**, *16*, 261.

(6) (a) Cheong, M.; Basolo, F. *Organometallics* **1988**, *7*, 2041. (b) Wang, D. M.; Angelici, R. J. *Inorg. Chem.* **1996**, *35*, 1321. (c) Nataro, C.; Thomas, L. M.; Angelici, R. J. *Inorg. Chem.* **1997**, *36*, 6000.

(7) (a) Witte, P.; Lal, T. K.; Waymouth, R. M. *Organometallics* **1999**, *18*, 4147. (b) Tagge, C. D.; Kravchenko, R. L.; Lal, T. K.; Waymouth, R. M. *Organometallics* **1999**, *18*, 380.

(8) (a) Batsanov, A. S.; Bridgewater, B. M.; Wilson, C. *J. Organomet. Chem.* **1999**, *590*, 169. (b) Halterman, R. L. *Chem. Rev.* **1992**, *92*, 965. (c) Möhring, P. C.; Coville, N. J. *J. Organomet. Chem.* **1994**, *479*, 1. (d) Hoveyda, A. H.; Morken, J. P. *Angew. Chem., Int. Ed. Engl.* **1996**, *35*, 1262.

(9) (a) Torrent, M.; Sola, M.; Frenking, G. *Chem. Rev.* **2000**, *100*, 439−493. (b) Gladysz, J. A.; Boone, B. J. *Angew. Chem., Int. Ed. Engl.* **1997**, *36*, 551−583. (c) Doucet, H.; Fernandez, E.; Layzell, T. P.; Brown, J. M. *Chem. Eur. J.* **1999**, *5*, 1320−1330.

(10) (a) Richardson, D. E.; Alameddin, N. G.; Ryan, M. F.; Hayes, T.; Eyler, J. R.; Siedle, A. R. *J. Am. Chem. Soc.* **1996**, *118*, 11244. (b) Alameddin, N. G.; Ryan, M. F.; Eyler, J. R.; Siedle, A. R.; Richardson, D. E. *Organometallics* **1995**, *14*, 5005. (c) Richardson, D. E. *Elect. Trans. React.* **1997**, *253*, 79. (d) Ryan, M. F.; Siedle, A. R.; Burk, M. J.; Richardson, D. E. *Organometallics* **1992**, *11*, 4231. (e) Kucht, A.; Kucht, H.; Song, W.; Rausch, M. D.; Chien, J. C. W. *Appl. Organomet. Chem.* **1994**, *8*, 437. (f) Schnabel, R. C.; Scott, B. L.; Smith, W. H.; Burns, C. J. *J. Organomet. Chem.* **1999**, *591*, 14. (g) Bursten, B. E.; Green, M. R. *Prog. Inorg. Chem.* **1988**, *36*, 393. (h) Slocum, D. W.; Ernst, C. R. *Adv. Organomet. Chem.* **1972**, *10*, 79. (i) Senoff, C. V. *Coord. Chem. Rev.* **1980**, *32*, 111. (j) King, R. B. *Coord. Chem. Rev.* **1976**, *20*, 155.

(11) (a) Blais, M. S.; Rausch, M. D. *J. Organomet. Chem.* **1995**, *502*, 1. (b) Rausch, M. D.; Lewison, J. F.; Hart, W. P. *J. Organomet. Chem.* **1988**, *358*, 161. (c) Hart, W. P.; Macomber, D. W.; Rausch, M. D. *J. Am. Chem. Soc.* **1980**, *102*, 1196.

(12) Möhring, P. C.; Coville, N. J. *J. Mol. Catal. A* **1995**, *96*, 181.

(13) Deck, P. A.; Jackson, W. F.; Fronczek, F. R. *Organometallics* **1996**, *15*, 5287.

(14) Deck, P. A.; Fronczek, F. R. *Organometallics* **2000**, *19*, 327.

(15) (a) Baschky, M. C.; Sowa, J. R.; Gassman, P. G.; Kass, S. R. *J. Chem. Soc., Perkin Trans. 2* **1996**, 213. (b) Burk, M. J.; Arduengo, A. J.; Calabrese, J. C.; Harlow, R. L. *J. Am. Chem. Soc.* **1989**, *111*, 8938.

(16) Blanchard, M. D.; Hughes, R. P.; Concolino, T. E.; Rheingold, A. L. *Chem. Mater.* **2000**, *12*, 1604.

(17) Richardson, D. E.; Lang, L.; Eyler, J. R.; Kircus, S. R.; Zheng, X. M.; Morse, C. A.; Hughes, R. P. *Organometallics* **1997**, *16*, 149.

(18) Maldanis, R. J.; Chien, J. C. W.; Rausch, M. D. *J. Organomet. Chem.* **2000**, *599*, 107.

(19) (a) Lehmus, P.; Kokko, E.; Härkki, O.; Leino. R.; Luttikhedde, H. J. G.; Nasman, J. H.; Seppälä, J. V. *Macromolecules* **1999**, *32*, 3547. (b) Plenio, H.; Burth, D. *Angew. Chem., Int. Ed. Engl.* **1995**, *34*, 800.

Electrochemical Studies. Single-sweep cyclic and Osteryoung square-wave voltammetric data were obtained for the sparingly soluble substituted ferrocenes **11** and **12** at nominal concentrations of about 2 μM in CH_2Cl_2 using 0.10 M [n-Bu_4N]-[PF_6] as the electrolyte and activated alumina as an internal desiccant. The substituted cobaltocenes **13**−**16** were analyzed similarly, using instead acetonitrile as the solvent. The apparatus was a BioAnalytical Systems BAS-100B automated digital potentiostat with a Pt-disk working electrode, a Pt wire auxiliary electrode, and a Ag/AgCl reference electrode. Cyclic voltammetric (CV) sweeps for substituted ferrocenes were typically initialized at +100 mV, scanned to +1100 mV, and reversed to +100 mV, at a scan rate 100 mV s^{-1}. CV sweeps for substituted cobaltocenium hexafluorophosphates were typically initialized at −100 mV, scanned to −1300 mV, and reversed to −100 mV, at a scan rate of 100 mV s^{-1}. $|E_{ox} - E_{red}|$ were less than 80 mV, and I_c/I_a ratios were within 15% of unity, both indicators of substantially reversible couples.

Shifts in oxidation potential of substituted ferrocenes were obtained by Osteryoung square-wave voltammetry (OSWV) using ferrocene as an internal standard. The cell voltage was typically swept from −200 to +1100 mV with a step resolution of 4 mV, a square wave-amplitude of 25 mV, and frequency of 15 Hz. Shifts in oxidation potentials of substituted cobaltocenes were similarly determined by OSWV using a sweep from −100 to −1300 mV and either octamethylferrocene or **9** as an internal standard.

Crystallographic Studies. Two crystalline polymorphs of **2a** were found under slightly different crystallization conditions. The first, **2a-i**, was obtained by cooling a moderately concentrated hexanes solution for 24 h in a refrigerator at 5 °C. The second, **2a-ii**, was obtained serendipitously during studies of the reaction of **2a** with dimethyl acetylenedicarboxylate (DMAD). These investigations will be reported in more detail elsewhere. One crude product mixture contained unreacted DMAD; unreacted **2a**; a product tentatively identified as 1,2-di(carbomethoxy)-3,5-bis(pentafluorophenyl)norbornadiene (a Diels−Alder adduct of DMAD), **2b**; and toluene (residual reaction solvent). Crystallization of this mixture from hexanes at −5 °C afforded **2a-ii**. No attempts were made to identify specific conditions that will lead predictably to the two different polymorphs of **2a**. Crystals of **4** were obtained by slow evaporation of a concentrated hexanes solution at 25 °C. Crystals of **11·4(C_6H_6)** were grown from benzene by slow evaporation. Crystals of **16** were obtained by slow evaporation of an *n*-octane solution at 25 °C. Crystals of **23·C_6D_6** were obtained by cooling a solution of **23** in C_6D_6 to 25 °C. Crystals of **26** were obtained by dissolving the complex in warm hexanes and cooling the solution to 0 °C for several days. Crystals of **27** were obtained by slow evaporation of a hexanes solution at 25 °C. No unusual procedures were required in the preparation of any of these crystals, except that the benzene solvates must be handled quickly after removal from their respective mother liquors. The single-crystal X-ray diffraction analyses (data collection, solution, and refinement) were unremarkable. Relevant crystallographic data are presented in Table 1.

Semiempirical Modeling. Calculations were carried out at the PM3 level of semiempirical theory using PC Spartan Pro software from Wavefunction, Inc. To map the conformational energies of 1,2-diarylcyclopentadienyl anions (aryl = Ph, C_6F_5), one aryl group was fixed at a given angle (0−90°, 5° intervals), and the remaining geometric parameters were energy-minimized. An analogous technique was used with 1,2,3-triarylcyclopentadienyl anions by fixing the torsion angle of the central aryl group. Plots of the minimized energies as a function of the fixed dihedral angle are provided in the Supporting Information.

1,2,4-Tris(pentafluorophenyl)cyclopentadiene (3). A mixture of lithium cyclopentadienide (0.790 g, 11.0 mmol), hexafluorobenzene (9.74 g, 52.3 mmol), NaH (1.36 g, 56.7 mmol), and diglyme (50 mL) was stirred at 110 °C for 14 h. The mixture was cooled and filtered through Celite, using 30 mL of THF to wash the filter. The filtrate was evaporated, and the residue was taken up in 50 mL of THF and added using a canulla to a stirred 10% aqueous NH_4Cl solution (250 mL). The mixture was stirred for 20 min and then rotary-evaporated until the organic solvents were removed. The resulting aqueous mixture was extracted with 150 mL of benzene. The organic layer was washed with water, dried over $MgSO_4$, filtered, and evaporated to afford a dark brown residue that was shown by ^{19}F NMR analysis to comprise a mixture of C_6F_5-substituted cyclopentadienes. The mixture was redissolved in about 1 L of hexanes, filtered through alumina to remove highly colored impurities, and evaporated. The resulting residue was taken up in about 25 mL of hexanes and filtered; the insoluble portion was pure **4** (see following procedure). The filtrate was loaded onto a 10 × 70 cm column of silica gel, which was eluted with hexanes. After a long forerun, an initial band afforded 1,4-bis(pentafluorophenyl)-cyclopentadiene (**2**). A subsequent band afforded 1.41 g (2.50 mmol, 23%) of **3** as an off-white solid. Mp: 106−108 °C. ^1H NMR ($CDCl_3$): δ 7.32 (s, 1 H), 4.14 (s, 2 H). ^{19}F NMR ($CDCl_3$): δ −141.03 (d, ^3J = 21 Hz, 2 F), −141.40 (d, ^3J = 22 Hz, 2 F), −141.56 (d, ^3J = 22 Hz, 2 F), −154.21 (t, ^3J = 21 Hz, 1 F), −154.41 (t, ^3J = 21 Hz, 1 F), −156.49 (t, ^3J = 21 Hz, 1 F), −162.30 (m, 4 F), −163.46 (m, 2 F). $\{^{19}F\}^{13}C$ NMR ($CDCl_3$): δ 144.6 (s, CF), 143.9 (s, CF), 143.8 (s, CF), 141.2 (s, CF), 141.0 (s, CF), 140.0 (s, CF), 138.0 (s, CF), 137.8 (s, CF), 137.8 (s, CF), 137.3 (d, J = 174 Hz, CH), 134.7 (t, J = 5 Hz, C−C_6F_5), 133.6 (m, 2 unresolved C−C_6F_5 signals), 110.3 (s, C_{ipso}), 110.1 (d, J = 2 Hz, C_{ipso}), 109.9 (s, C_{ipso}), 47.7 (td, J = 132 Hz, J = 8 Hz, CH_2). $\{^1H\}^{13}C$ NMR ($CDCl_3$): δ 144.7 (d, J = 247 Hz, CF), 144.0 (d, J = 246 Hz, CF), 141.1 (d, J = 251 Hz, CF), 140.0 (d, J = 256 Hz, CF), 138.0 (d, J = 244, CF), 137.9 (d, J = 247 Hz, CF), 137.8 (d, J = 262, CF), 137.3 (t, J = 8 Hz, CH), 134.7 (m, C−C_6F_5), 133.5 (s, 2 unresolved C−C_6F_5 signals), 110.2 (m, C_{ipso}), 110.1 (d, J = 4 Hz, C_{ispo}), 109.9 (m, C_{ipso}), 47.7 (s, CH_2). Anal. Calcd for $C_{23}H_3F_{15}$: C, 48.96; H, 0.54. Found: C, 49.02; H, 0.35.

1,2,3-Tris(pentafluorophenyl)cyclopentadiene (4). From the chromatographic separation described in the synthesis of **3**, a third band was eluted to afford 1.04 g (1.84 mmol, 17%) of **4** as an off-white crystalline solid. Mp: 216−217 °C. This yield includes the solid obtained in the filtration immediately prior to the chromatographic separation (see above). ^1H NMR ($CDCl_3$): δ 6.97 (t, J = 1.5 Hz, 1 H), 3.80 (d, J = 1.2 Hz, 2 H). ^{19}F NMR ($CDCl_3$): δ −141.61 (m, 4 F), −142.11 (d, ^3J = 23 Hz, 2 F), −153.24 (t, ^3J = 21 Hz, 1 F), −154.27 (t, ^3J = 20 Hz, 1 F), −154.66 (t, ^3J = 21 Hz, 1 F), −161.76 (m, 2 F), −162.22 (m, 2 F), −162.56 (m, 2 F). $\{^{19}F\}^{13}C$ NMR ($CDCl_3$): δ 144.1 (s, CF), 143.9 (s, CF), 143.7 (s, CF), 141.2 (s, CF), 141.0 (s, CF), 140.9 (s, CF), 139.7 (d, J = 175 Hz, CH), 137.8 (s, CF), 137.6 (s, CF), 137.4 (s, CF), 134.4 (m, C−C_6F_5), 133.9 (m, C−C_6F_5), 132.3 (m, C−C_6F_5), 110.0 (s, C_{ipso}), 109.5 (d, J = 2 Hz, C_{ispo}), 108.9 (s, C_{ipso}), 45.6 (td, J = 134 Hz, J = 8 Hz, CH_2). $\{^1H\}^{13}C$ NMR ($CDCl_3$): δ 143.8 (br d, 3 unresolved CF), 141.1 (br d, J = 284 Hz, 3 unresolved CF), 139.7 (s, CH), 137.6 (br d, 3 unresolved CF), 134.4 (s, C−C_6F_5), 133.9 (m, C−C_6F_5), 132.3 (s, C−C_6F_5), 45.5 (s, CH_2); the three C_{ipso} signals were not observed. Anal. Calcd for $C_{23}H_3F_{15}$: C, 48.96; H, 0.54. Found: C, 49.21; H, 0.48.

Sodium 1,2,4-Tris(pentafluorophenyl)cyclopentadienide (7). A mixture of 1,2,4-tris(pentafluorophenyl)cyclopentadiene (**3**, 3.04 g, 5.39 mmol), NaH (0.75 g, 31 mmol), and THF (50 mL) was stirred at 25 °C for 1 day. The mixture was filtered to remove unreacted NaH, and the filtrate was evaporated. The residue was triturated with hexane, collected on a fritted filter, and dried under vacuum at 80 °C to yield 2.99 g (5.10 mmol, 95%) of a tan solid. ^1H NMR (THF-d_8): δ 6.71 (2 H). ^{19}F NMR (THF-d_8): δ −146.64 (d, ^3J = 22 Hz, 4 F), −148.01 (d, ^3J = 18 Hz, 2 F), −169.36 (t, ^3J = 20 Hz, 4 F), −169.82 (tt, ^3J = 21 Hz, ^4J = 3 Hz, 2 F), −170.09 (m, 2 F),

Table 1. Crystallographic Data

	2-i	**2-ii**	**4**	**11**·4C_6H_6
empirical formula	$C_{17}H_4F_{10}$	$C_{17}H_4F_{10}$	$C_{23}H_3F_{15}$	$C_{46}H_4F_{30}Fe$·4C_6H_6
fw	398.20	398.20	564.26	1494.77
diffractometer	Enraf-Nonius CAD4	Siemens P4	Enraf-Nonius CAD4	Enraf-Nonius Kappa CCD
cryst dimens (mm)	0.22 × 0.28 × 0.48	0.44 × 0.34 × 0.15	0.30 × 0.30 × 0.10	0.12 × 0.15 × 0.25
cryst system	monoclinic	monoclinic	tetragonal	triclinic
a (Å)	14.5190(10)	13.1079(10)	7.4767(9)	11.7507(4)
b (Å)	5.0173(3)	13.7150(11)	7.4767(9)	13.1551(4)
c (Å)	20.5780(10)	8.3515(7)	35.794(2)	20.7085(6)
α (deg)	90	90	90	84.443(2)
β (deg)	108.009(7)	105.812(7)	90	78.008(2)
γ (deg)	90	90	90	70.1770(10)
V (Å)^3	1425.6(2)	1444.6(2)	2000.9(6)	2944.41(16)
space group	$P2_1/c$	$P2_1/c$	$P4_12_12$	$P\bar{1}$
Z	4	4	4	2
D_{calc} (Mg m^{-3})	1.855	1.831	1.869	1.686
abs coeff (mm^{-1})	1.8	0.197	0.199	0.4
F_{000}	784	784	1104	1488
radiation	Cu K	Mo K	Mo K	Mo K
(K) (Å)	1.54184	0.71073	0.71073	0.71073
temp (K)	297	293	103	100
range for collection	0.0−74.9	1.61−24.99	0.0−31.0	0.0−30.0
no. of reflns colld	3418	3082	7175	16 606
no. of indep reflns	2934	2513	2070	16 603
abs corr method	empirical	integration	none	empirical
max, min transm	1.00, 0.89	0.95, 0.93		0.95, 0.92
data/restrts/params	2606/0/261	2531/0/261	1820/0/187	16603/0/910
R [$I > 2\sigma(I)$]	0.037	0.0374	0.047	0.040
R_w [$I > 2\sigma(I)$]	0.052	0.0788	0.060	0.078
GoF on F^2	3.029	0.732	0.949	0.762
largest diff peak, hole (e Å^{-3})	0.20, −0.16	0.13, −0.12	0.25, −0.20	0.58, −0.42

	16	**23**·1/2C_6D_6	**26**	**27**
empirical formula	$C_{46}H_4CoF_{30}$	$C_{26}H_2F_{15}MnO_3$·1/2C_6D_6	$C_{20}H_3F_{10}O_3Re$	$C_{26}H_2F_{15}O_3Re$
fw	1185.42	744.29	667.43	833.48
diffractometer	Siemens P4	Siemens P4	Enraf-Nonius CAD4	Siemens P4
cryst dimens (mm)	0.51 × 0.16 × 0.08	0.48 × 0.49 × 0.32	0.18 × 0.25 × 0.30	0.17 × 0.19 × 0.48
cryst system	monoclinic	triclinic	triclinic	monoclinic
a (Å)	7.5933(8)	7.0264(13)	7.4561(8)	7.6570(7)
b (Å)	14.2469(15)	13.269(3)	10.0723(8)	10.8461(10)
c (Å)	38.263(4)	15.229(3)	13.1941(13)	29.606(2)
α (deg)	90	105.837	83.379(7)	90
β (deg)	91.728(8)	99.893	74.710(9)	92.696(7)
γ (deg)	90	93.846	89.520(8)	90
V (Å)^3	4137.5(7)	1335.9(4)	949.18(16)	2452.8(4)
space group	$P2_1/c$ (No. 14)	$P\bar{1}$ (No. 2)	$P\bar{1}$ (No. 2)	$P2_1/c$ (No. 14)
Z	4	2	2	4
D_{calc} (Mg m^{-3})	1.903	1.850	2.335	2.257
abs coeff (mm^{-1})	0.588	0.633	6.603	5.100
F_{000}	2308	726	624	1568
radiation	Mo Kα	Mo Kα	Mo Kα	Mo Kα
λ (Å)	0.71073	0.71073	0.71073	0.71073
temp (K)	293(2)	293(2)	293(2)	293(2)
θ range for collection	1.06−21.50	1.81−25.00	0.0−30.4	2.00−26.00
no. of reflns colld	6508	5919	11496	6677
no. of indep reflns	4752	4670	5748	4828
abs corr method	integration	*ψ*-scans	*ψ*-scans	integration
max, min transm	0.9667, 0.9052	0.6518, 0.5727	0.9966, 0.7654	0.6235, 0.5067
no. of data/restrts/params	4750/0/694	4670/0/441	4463/0/308	4826/0/406
R [$I > 2\sigma(I)$]	0.0467	0.0454	0.0490	0.0348
R_w [$I > 2\sigma(I)$]	0.1054	0.1159	0.0590	0.0986
GoF on F^2	0.915	1.000	1.680	0.896
diff peak, hole (e Å^{-3})	0.266, −0.319	0.449, −0.418	2.11, −0.43	1.052, −1.358

−175.29 (tt, ^3J = 21 Hz, ^4J = 5 Hz, 1 F). {^{19}F}^{13}C NMR (THF-d_8): *δ* 143.5 (s, CF), 143.0 (s, CF), 137.9 (s, CF), 137.6 (s, CF), 136.3 (s, CF), 118.9 (s, CF), 117.6 (s, C_{ipso}), 115.2 (d, J = 165 Hz, CH), 107.0 (m, *C*−C_6F_5), 105.3 (m, *C*−C_6F_5). {^{1}H}^{13}C NMR (THF-d_8): *δ* 143.0 (d, J = 240 Hz, CF), 143.0 (d, J = 243 Hz, CF), 138.0 (d, J = 242 Hz, CF), 137.6 (d, J = 220 Hz, CF), 136.4 (d, J = 240 Hz, CF), 133.9 (d, J = 234 Hz, CF), 118.9 (t, J = 18 Hz, C_{ipso}), 117.6 (t, J = 15 Hz, C_{ipso}), 115.2 (s, CH), 107.0 (s, *C*−C_6F_5), 105.3 (s, *C*−C_6F_5).

Sodium 1,2,3-Tris(pentafluorophenyl)cyclopentadienide (8). The procedure for the synthesis of **7** was followed, using instead 1,2,3-tris(pentafluorophenyl)cyclopentadiene (**4**, 1.73 g, 3.07 mmol) and NaH (0.41 g, 17 mmol) as the starting materials to obtain 1.53 g (2.62 mmol, 85%) of tan solid. ^{1}H NMR (THF-d_8): *δ* 6.16 (s, 2 H). ^{19}F NMR (THF-d_8): *δ* −144.15 (d, ^3J = 20 Hz, 2 F), −144.45 (d, ^3J = 22 Hz, 4 F), −166.14 (tt, ^3J = 21 Hz, ^4J = 2 Hz, 1 F), −167.40 (m, 6 F), −168.12 (tt, ^3J = 21 Hz, ^4J = 3 Hz, 2 F). {^{19}F}^{13}C NMR (THF-d_8): *δ* 145.7 (s, CF), 145.4 (s, CF), 139.4 (s, CF), 139.2 (s, CF), 138.8 (CF), 138.1 (CF), 120.7 (s, C_{ipso}), 113.9 (d, J = 166 Hz, 2 CH), 107.2 (t, J = 7.6 Hz, *C*−C_6F_5), 105.2 (s, *C*−C_6F_5); no signal that we could assign to the second C_{ipso} was observed. {^{1}H}^{13}C NMR (THF-

d_8): δ 145.7 (d, J = 240 Hz, CF), 145.4 (d, J = 240 Hz, CF), 139.4 (m, 2 unresolved CF), 138.8 (d, J = 246 Hz, CF), 138.1 (d, J = 243 Hz, CF), 120.7 (t, J = 20 Hz, C_{ipso}), 113.9 (s, CH), 107.2 (s, $C-C_6F_5$), 105.2 (s, $C-C_6F_5$); no signal that we could assign to the second C_{ipso} was observed.

Bis[η^5-1,2,4-tris(pentafluorophenyl)cyclopentadienyl]-iron(II) (11). A mixture of sodium 1,2,4-tris(pentafluorophenyl)cyclopentadienide (**7**, 0.493 g, 0.841 mmol), $FeBr_2$ (0.095 g, 0.44 mmol), and THF (50 mL) was refluxed for 1 day, and then the solvent was evaporated. The residue was extracted with hot toluene (50 mL) and filtered, and the filtrate was evaporated. The resulting orange solid was washed with pentane (50 mL) on a fritted filter to afford 0.284 g (0.24 mmol, 57%) of an orange solid. ^{1}H NMR (THF-d_8): δ 5.61 (s, 4 H). ^{19}F NMR (THF-d_8): δ −137.36 (br s, 8 F), −138.84 (d, ^3J = 16 Hz, 4 F), −155.08 (t, ^3J = 20 Hz, 4 F), −156.78 (t, ^3J = 20 Hz, 2 F), −163.11 (m, 8 F), −163.92 (m, 4 F). Anal. Calcd for $C_{46}H_4F_{30}Fe$: C, 46.73; H, 0.34. Found: C, 46.62; H, 0.16.

Bis[η^5-1,2,3-tris(pentafluorophenyl)cyclopentadienyl]-iron(II) (12). A mixture of sodium 1,2,3-tris(pentafluorophenyl)cyclopentadienide (**8**, 0.305 g, 0.520 mmol), $FeBr_2$ (0.052 g, 0.243 mmol), and THF (25 mL) was refluxed for 1 day. The THF was then evaporated. The residue was extracted with hot toluene (25 mL), filtered, and cooled to 25 °C to afford 0.100 g (0.084 mmol, 35%) of orange crystals. ^{1}H NMR (THF-d_8): δ 5.63 (s, 4 H). ^{19}F NMR (THF-d_8): δ −134.82 (s, 2 F), −137.33 (br s, 8 F), −140.69 (d, ^3J = 24 Hz, 2 F), −153.96 (t, ^3J = 21 Hz, 2 F), −155.27 (t, ^3J = 20 Hz, 4 F), −162.17 (m, 2 F), −163.14 (m, 10 F). Anal. Calcd for $C_{46}H_4F_{30}Fe$: C, 46.73; H, 0.34. Found: C, 46.50; H, 0.24.

1,1′-Bis(pentafluorophenyl)cobaltocene (13). A solution of anhydrous cobalt(II) bromide (219 mg, 1.00 mmol) and sodium (pentafluorophenyl)cyclopentadienide (**5**, 508 mg, 2.00 mmol) in THF was refluxed for 2 h and then cooled. The solvent was evaporated, and the dark residue was extracted with 50 mL of toluene and filtered. The dark filtrate was evaporated to afford a violet-black solid, which was subsequently recrystallized from pentane at −20 °C to afford 405 mg (0.777 mmol, 78%) of violet crystals. An analytical sample was obtained by sublimation (100−120 °C, 0.050 Torr). ^{1}H NMR (THF-d_8): δ 29.1 (br), −44.9 (br). Anal. Calcd for $C_{22}H_8F_{10}Co$: C, 50.70; H, 1.55. Found: C, 50.52; H, 1.61.

Bis[η^5-1,3-bis(pentafluorophenyl)cyclopentadienyl]-cobalt(II) (14). A mixture of **6** (0.500 g, 1.20 mmol), $CoBr_2$ (0.130 g, 0.600 mmol), and THF (100 mL) was stirred for 0.5 h at 25 °C, and then the solvent was then evaporated. Under air, the residue was dissolved in 1 L of benzene, washed with 50 mL of 1.0 M aqueous HCl, then water (3 × 50 mL), dried over $MgSO_4$, filtered, and evaporated. The resulting solid was triturated with pentane (3 × 50 mL) and dried under vacuum to afford 410 mg (0.48 mmol, 80%) of a deep indigo microcrystalline solid. In CD_2Cl_2 solution, the ^{1}H NMR spectrum showed no signals, whereas ^{19}F NMR showed a set of two broad (fwhm ≈ 10 000 Hz), unresolved signals at about −160 and −175 ppm. Anal. Calcd for $C_{34}H_6F_{20}Co$: C, 47.83; H, 0.71. Found: C, 48.09; H, 0.77.

Bis[η^5-1,2,4-tris(pentafluorophenyl)cyclopentadienyl]-cobalt(II) (15). A mixture of **7** (0.494 g, 0.843 mmol), $CoBr_2$ (0.093, 0.425 mmol), and THF (25 mL) was refluxed for 1 day, cooled, and filtered. Evaporation of the filtrate afforded a violet solid, which was triturated with toluene, collected on a filter, and dried under vacuum to afford 0.337 g (0.284 mmol, 67%) of a purple solid. ^{1}H NMR (THF-d_8): δ 1.7 (br s). ^{19}F NMR (THF-d_8): δ −84.60 (br s, 4 F), −100.76 (br s, 10 F), −129.73 (s, 4 F), −163.09 (s, 8 F), −179.62 (s, 4 F). Anal. Calcd for $C_{46}H_4F_{30}Co$: C, 46.73; H, 0.34. Found: C, 46.58; H, 0.05.

Bis[η^5-1,2,3-tris(pentafluorophenyl)cyclopentadienyl]-cobalt(II) (16). A mixture of **8** (0.265 g, 0.422 mmol), $CoBr_2$ (0.047 g, 0.215 mmol), and THF (50 mL) was refluxed for 1 day, cooled, and filtered. Evaporation of the filtrate afforded a violet solid, which was triturated with hexanes, collected on a filter, and dried to afford 0.086 g (0.072 mmol, 34%) of a purple solid. ^{1}H NMR (THF-d_8): δ −20.5 (br s). ^{19}F NMR (THF-d_8): δ −43.3 (s, 2 F), −84.4 (br s, 8 F), −125.8 (s, 4 F), −142.5 (s, 2 F), −144.0 (s, 2 F), −146.2 (t, ^3J = 21 Hz, 2 F), −160.3 (br s, 8 F), −163.0 (s, 2F). Anal. Calcd for $C_{46}H_4F_{30}Co$: C, 46.73; H, 0.34. Found: C, 46.58; H, 0.05.

Bis[η^5-(pentafluorophenyl)cyclopentadienyl]cobalt-(III) Hexafluorophosphate (17). Air was bubbled through a biphasic mixture of **13** (148 mg, 0.284 mmol), toluene (50 mL), water (50 mL), and 12 M aqueous HCl (20 mL) until the dark color of the starting material in the organic phase disappeared. The layers were separated, and the crude product was precipitated with aqueous KPF_6, collected on a filter, and dried in a vacuum desiccator over anhydrous calcium sulfate to afford 161.9 mg (0.243 mmol, 86%) of a yellow powder. ^{1}H NMR (acetone-d_6): δ 6.52 (t, $^3J_{HH}$ = 2.0 Hz, 4 H), 6.27 (t, $^3J_{HH}$ = 2.1 Hz, 4 H). ^{19}F NMR (acetone-d_6): δ −68.50 (d, $^1J_{PF}$ = 707 Hz, 6 F), −133.49 (d, $^3J_{FF}$ = 19 Hz, 2 F), −149.21 (tt, $^3J_{FF}$ = 21 Hz, $^5J_{FH}$ = 4 Hz, 4 F), −158.99 (m, 4 F). {^{1}H}^{13}C NMR (acetone-d_6): δ 146.2 (d, $^1J_{CF}$ = 243 Hz), 142.9 (d, $^1J_{CF}$ = 259 Hz), 139.2 (d, $^1J_{CF}$ = 251 Hz), 106.6 (s), 91.7 (s), 88.1 (s), 86.6 (t, $^2J_{CF}$ = 3 Hz). Anal. Calcd for $C_{22}H_8F_{16}PCo$: C, 39.66; H, 1.21. Found: C, 39.35; H, 1.11.

Bis{bis[η^5-1,3-bis(pentafluorophenyl)cyclopentadienyl]-cobalt(III)} Sulfate (18). In a 15 mL test tube fitted with a stir bar, concentrated sulfuric acid (1 mL) was added to 40.0 mg of **14**, and the mixture was stirred for 2 h at 25 °C. Using a pipet, the resulting orange solution was added dropwise to 10 g of ice and then stirred until the ice melted. The yellow precipitate was collected on a filter and washed with 10 mL of water (upon which an indigo color suggesting partial reduction to **14** had occurred) and ether (3 × 10 mL). The dark precipitate was dissolved in 5 mL of acetone, filtered, reprecipitated in 100 mL of rapidly stirred anhydrous ether, collected on a filter, and then dried in a vacuum oven at 60 °C for 4 h to obtain 28 mg of a black-yellow solid. ^{1}H NMR (acetone-d_6): δ 6.9 (br s, 4 H), 6.8 (br s, 2 H). ^{19}F NMR (acetone-d_6): δ −137.5 (m, 8 F), −152.9 (m, 4 F), −163.6 (m, 8 F). Satisfactory microanalytical data were not obtained.

Tricarbonyl[η^5-pentafluorophenylcyclopentadienyl]-manganese(I) (21). A mixture of $Mn(CO)_5Br$ (0.42 g, 1.5 mmol), $(C_6F_5C_5H_4)Na$ (**5**, 0.42 g, 1.6 mmol), and THF (50 mL) was refluxed for 1 day. The THF was evaporated, and the resulting crude solid was dissolved in hexane and filtered. The filtrate was cooled to −20 °C for 1 day, and 0.38 g (1.0 mmol, 67%) of a yellow solid was collected. IR (hexane): ν_{CO} (cm^{-1}) = 2032 (A_1), 1954 (E). ^{1}H NMR (C_6D_6): δ 4.67 (pentet, J = 2.0 Hz, 2 H), 3.87 (t, J = 2.2 Hz, 2 H). ^{19}F NMR (C_6D_6): δ −139.56 (dd, ^3J = 22.0 Hz, ^5J = 5.5 Hz, 2 F), −155.50 (t, ^3J = 22.2 Hz, 1 F), −162.33 (m, 2 F). Anal. Calcd for $C_{14}H_4F_5MnO_3$: C, 45.43; H, 1.09. Found: C, 45.64; H, 0.95.

Tricarbonyl[η^5-1,3-bis(pentafluorophenyl)cyclopentadienyl]manganese(I) (22). A mixture of $Mn(CO)_5Br$ (0.23 g, 0.84 mmol), $[1,3-(C_6F_5)_2C_5H_3]Na$ (**6**, 0.36 g, 0.86 mmol), and THF (50 mL) was stirred under reflux for 2 days. The THF was then evaporated, and the resulting crude solid was dissolved in hexane and filtered. Cooling the filtrate to −78 °C for about 5 h precipitated the product, which was collected on a filter and dried under vacuum to afford 0.31 g (0.58 mmol, 69%) of a yellow solid. IR (hexane): ν_{CO} (cm^{-1}) 2035 (A_1), 1966, 1960. ^{1}H NMR (C_6D_6): δ 5.65 (pentet, J = 1.3 Hz, 1 H), 4.76 (s, 2 H). ^{19}F NMR (C_6D_6): δ −139.34 (d, ^3J = 18.0 Hz, 4 F), −154.24 (tt, ^3J = 21.8 Hz, 2 F), −161.66 (m, 4 F). Anal. Calcd for $C_{20}H_3F_{10}MnO_3$: C, 44.80; H, 0.56. Found: C, 45.03; H, 0.37.

Tricarbonyl[η^5-1,2,4-tris(pentafluorophenyl)cyclopentadienyl]manganese(I) (23). A mixture of $Mn(CO)_5Br$ (0.102 g, 0.371 mmol), $[1,2,4-(C_6F_5)_3C_5H_2]Na$ (**7**, 0.224 g, 0.382 mmol), and THF (20 mL) was refluxed for 1 day. The THF was evaporated, and the resulting crude solid was recrystallized from hexanes to afford 0.065 g (0.093 mmol, 25%) of an orange crystalline solid. IR (hexane): ν_{CO} (cm^{-1}) 2040 (A_1), 1973, 1965.

^{1}H NMR (C_6D_6): δ 5.51 (s, 2 H). ^{19}F NMR (C_6D_6): δ −137.37 (d, ^3J = 18 Hz, 4 F), −140.24 (d, ^3J = 18 Hz, 2 F), −152.17 (d, ^3J = 22 Hz, 2 F), −154.20 (t, ^3J = 22 Hz, 1 F), −161.66 (td, ^3J = 23 Hz, ^5J = 7 Hz, 4 F), −162.10 (m, 2 F). Anal. Calcd for $C_{26}H_2F_{15}MnO_3$: C, 44.47; H, 0.29. Found: C, 44.32; H, 0.12.

Tricarbonyl[η^5-1,2,3-tris(pentafluorophenyl)cyclopentadienyl]manganese(I) (24). A mixture of $Mn(CO)_5Br$ (0.104 g, 0.378 mmol), [1,2,3-$(C_6F_5)_3C_5H_2$]Na (0.227 g, 0.387 mmol), and THF (20 mL) was stirred under reflux for 1 day. The THF was evaporated, and the resulting crude solid was recrystallized from toluene at −78 °C to afford 0.124 g (0.176 mmol, 47%) of an orange solid. IR (hexane): ν_{CO} (cm^{-1}) 2041 (A_1), 1975, 1963. ^{1}H NMR (C_6D_6): δ 4.47 (s, 1 H). ^{19}F NMR (C_6D_6): δ −131.13 (d, ^3J = 22 Hz, 1 F), −137.13 (d, ^3J = 18 Hz, 4 F), −141.14 (d, ^3J = 23 Hz, 1 F), −150.34 (t, ^3J = 22 Hz, 1 F), −151.83 (t, ^3J = 22 Hz, 2 F), −160.61 (td, ^3J = 22 Hz, ^5J = 7 Hz, 1 F), −161.51 (td, ^3J = 23 Hz, ^5J = 8 Hz, 4 F), −161.76 (td, ^3J = 22 Hz, ^5J = 8 Hz, 1 F). Anal. Calcd for $C_{26}H_2F_{15}MnO_3$: C, 44.47; H, 0.29. Found: C, 44.07; H, 0.17.

Tricarbonyl[η^5-1,2,4-tris(pentafluorophenyl)cyclopentadienyl]rhenium(I) (27). A mixture of $Re(CO)_5Br$ (0.149 g, 0.367 mmol), **7** (0.225 g, 0.384 mmol), and THF (20 mL) was stirred under reflux for 1 day, and then the solvent was evaporated. The residue was dissolved in hexane and filtered through a pad of neutral alumina. The filtrate was evaporated, and the residue was recrystallized from methanol to yield 0.153 g (0.184 mmol, 50%) of a tan solid. IR (octane): ν_{CO} (cm^{-1}) 2042 (A_1), 1963, 1957. ^{1}H NMR ($CDCl_3$): δ 6.36 (s, 2 H). ^{19}F NMR ($CDCl_3$): δ −136.42 (s, 4 F), −139.22 (d, ^3J = 15 Hz, 2 F), −152.22 (t, ^3J = 21 Hz, 2 F), −153.95 (t, ^3J = 21 Hz, 1 F), −161.00 (m, 4 F), −161.46 (m, 2 F). Anal. Calcd for $C_{26}H_2F_{15}O_3Re$: C, 37.47; H, 0.24. Found: C, 37.65; H, 0.08.

Tricarbonyl[η^5-1,2,3-tris(pentafluorophenyl)cyclopentadienyl]rhenium(I) (28). A mixture of $Re(CO)_5Br$ (57.5 mg, 0.142 mmol), **8** (81.0 mg, 0.138 mmol), sodium hydride (35 mg, 1.4 mmol), and toluene (25 mL) was stirred at 105 °C for 24 h, and then the hot mixture was filtered. The filtrate was evaporated, and the residue was triturated with hexanes and collected on a filter to afford 50 mg (0.060 mmol, 43%) of a tan solid. IR (octane): ν_{CO} (cm^{-1}) 2043 (A_1), 1965, 1954. ^{1}H NMR ($CDCl_3$): δ 5.87 (s, 2 H). ^{19}F NMR ($CDCl_3$): δ −130.53 (m, 1 F), −135.96 (d, ^3J = 22 Hz, 4 F), −140.79 (d, $^3J_{FF}$ = 24 Hz, 1 F), −150.40 (t, $^3J_{FF}$ = 21 Hz, 1 F), −151.75 (t, J = 24 Hz, 2 F), −159.80 (m, 1 F), −160.72 (m, 5 F). Anal. Calcd for $C_{26}H_2F_{15}O_3Re$: C, 37.47; H, 0.24. Found: C, 37.27; H, 0.20.

Observation of Cobaltocenium Ions. To about 10 mg each of cobaltocenes **14**, **15**, and **16** in three separate 5 mm NMR tubes was added about 1.0 mL each of D_2SO_4. The tubes were capped and shaken occasionally over 20 min. The cobaltocene complexes appeared to dissolve completely to afford faintly turbid yellow-orange solutions of **18**, **19**, and **20**, respectively. The samples were subjected to ^{1}H and ^{19}F NMR spectroscopic analysis in D_2SO_4 solvent referenced to the residual solvent isotopomer ($HDSO_4$) at 10.90 ppm. Due to the viscosity of the sulfuric acid solvent, all of the NMR spectra exhibited sufficient broadening to preclude observation of spin−spin couplings, so no multiplicity information is presented. Data for **18**: ^{1}H NMR (D_2SO_4): 6.86 (2 H), 6.64 (2 H). ^{19}F NMR (D_2SO_4): −140.7 (8 F), −151.0 (4 F), −163.0 (8 F). Data for **19**: ^{1}H NMR (D_2SO_4): δ 6.77 (4 H). ^{19}F NMR (D_2SO_4): δ −138.2 (4 F), −138.5 (8 F), −147.8 (2 F), −148.9 (4 F), −161.4 (8 F), −161.9 (4 F). Data for **20**: ^{1}H NMR (D_2SO_4): δ 6.80 (4 H). ^{19}F NMR (D_2SO_4): δ −137.8 (2 F), −138.5 (8 F), −141.9 (2 F), −148.2 (4 F), −148.6 (2 F), −160.4 (2 F), −160.9 (10 F).

Results and Discussion

Ligand Syntheses. As shown in Scheme 1, sodium cyclopentadienide (NaCp) reacts with hexafluorobenzene (C_6F_6) to afford mixtures of mono-, di-, and triarylated cyclopentadienes. The arylation reaction presumably occurs via formal nucleophilic aromatic substitution. Product yields as a function of solvent, reaction temperature, and reaction time are summarized in Table 2. A large excess of C_6F_6 was used in all reactions. The choice of either lithium or sodium as the counterion for the starting material made no significant difference in the observed product ratios or isolated yields. Extended reaction times using diglyme as the solvent (entries 6 and 7) gave the best selectivity for the triarylated products. Although significant decomposition to dark, intractible byproducts decreased the isolated yields, the benefit of this procedure is the ability to isolate appreciable amounts of both regioisomers from a simple, inexpensive, one-pot procedure.

Compounds **1**−**4** are separated by silica gel chromatography and isolated as colorless, crystalline solids. Comparisons of crude yields determined by ^{1}H NMR (entries 2 and 4) with isolated, purified compounds (entries 3 and 5) show that the separation procedure is relatively inefficient. Chromatography is impeded by the sparing solubility of **3** and **4**. As we noted earlier, (pentafluorophenyl)cyclopentadiene (**1**) is obtained as a mixture of double-bond regioisomers and dimerizes slowly at room temperature.[13] The Supporting Information contains an improved procedure for isolating **1** using a cold aqueous workup to minimize dimerization. The diarylated cyclopentadiene **2** forms two double-bond isomers. One isomer (**2a**) has time-averaged C_{2v} symmetry, while the other isomer (**2b**) has C_s symmetry, enabling structural differentiation by ^{1}H and ^{19}F NMR spectroscopy. The isomers **2a** and **2b** coelute in our chromatographic procedure. The structure of **2a** is confirmed by crystallographic analysis (see below). Upon standing for several weeks, crystalline **2a** will slowly convert to a mixture of **2a** and **2b**. No effort has yet been made to study this interconversion in detail. A mixture of **2a** and **2b** is converted to the common conjugate base **6** upon treatment with NaH.

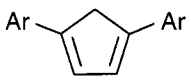

2a

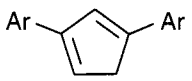

2b

Both of the two triarylated regioisomers **3** and **4** exhibit time-averaged C_s symmetry in solution. In the 1,2,4-isomer **3** both the CH_2 and CH protons are adjacent to *two* electron-withdrawing C_6F_5 groups, whereas in the 1,2,3-isomer **4**, the CH_2 and CH groups are each adjacent to only *one* C_6F_5 group. Accordingly, **3** shows ^{1}H NMR chemical shifts for the CH_2 (4.11 ppm) and CH (7.29 ppm), downfield of the corresponding signals (CH_2, 3.80 ppm; CH, 6.97 ppm) in the spectrum of the 1,2,3 isomer **4**. Furthermore, only **4** exhibits CH−CH_2 coupling ($J \approx 1.5$ Hz). This regiochemical assignment is confirmed by an X-ray diffraction analysis of crystalline **4** (see below). Regioselectivity in the formation of the triarylated cyclopentadienes **3** and **4** is minimal (Table 2).

Both triarylated cyclopentadienes **3** and **4** are converted efficiently to their corresponding sodium salts **7** and **8**, respectively, under similar deprotonation conditions (Scheme 1). The triarylated sodium cyclopentadienides **7** and **8** both demonstrated C_{2v} symmetry in THF

Scheme 1

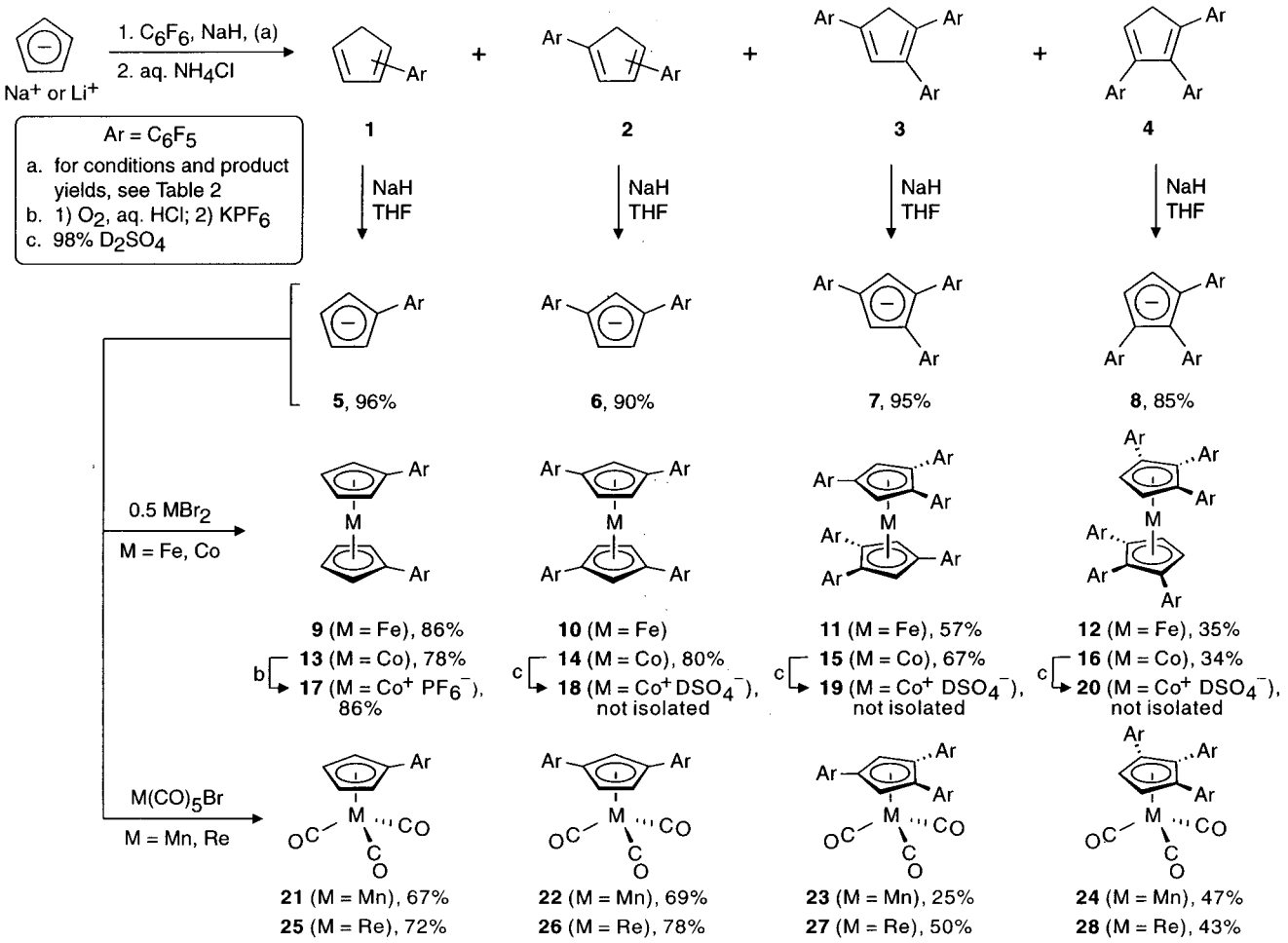

Table 2. Conditions and Yields of C_6F_5-Substituted Cyclopentadiene Syntheses

	reaction conditions			isolated yields (% based on NaCp)			
entry	solvent	*T* (°C)	time (h)	**1**	**2**	**3**	**4**
1.	DME	85	12	9	19	10	10
2.	DME	85	24	2[a]	26[a]	22[a]	19[a]
3.	DME	85	24	0	17	5	11
4.	DME	85	96	0[a]	6[a]	32[a]	20[a]
5.	DME	85	96	0	8	18	8
6.	diglyme	110	14	0	3	23	17
7.	diglyme	110	25	0	1	22	14

[a] ^{1}H NMR yields determined from the crude product mixture prior to separation.

solution on the basis of the number and intensity of signals in their ^{1}H and ^{19}F NMR spectra. Like the mono- and diarylated ligand salts **5** and **6** that we reported earlier, the triarylated salts **7** and **8** remain partly solvated by small but significant amounts of THF (up to 10 mol %) even after heating to 80 °C under high vacuum for several hours.

In our preliminary explorations of the synthesis of C_6F_5-substituted cyclopentadienes,[13] we dismissed many small, poorly reproducible NMR signals as arising from "minor impurities" (such as the disubstituted diene isomer **2b** without pursuing their assignments. Recently, we also learned that two additional compounds observed in some reactions are the vicinally disubstituted regioisomer **D** and the tetrasubstituted cyclopentadiene **E**. The isolation and characterization of **D** and **E**, along with their use as ligands for transition metals, are underway.

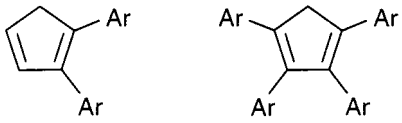

D **E**

Synthesis of Pentafluorophenyl-Substituted Ferrocenes. As Scheme 1 shows, reactions of iron(II) bromide with 2 equiv of an arylated cyclopentadienide ligand (**5**−**8**) afford the corresponding ferrocene complexes **9**−**12**, which are isolated as air-stable, red-orange solids. We reported the diarylated and tetraarylated ferrocenes **9** and **10** earlier,[13] and the structure of **9** was also reported elsewhere.[16] Although ferrocene is highly soluble in hydrocarbons, **9** is noticeably less soluble, and **10** is only sparingly soluble. The hexaarylated complexes **11** and **12** are essentially insoluble in hydrocarbons at room temperature, nor are they appreciably soluble in "fluorous" solvents including hexafluorobenzene,[20] but they are sufficiently soluble in THF-d_8 for ^{1}H and ^{19}F NMR measurements.

Synthesis of Pentafluorophenyl-Substituted Cobaltocenes. The syntheses of the substituted cobaltocenes are analogous to those of the ferrocenes (Scheme

(20) (a) Barthel-Rosa, L. P.; Gladysz, J. A. *Coord. Chem. Rev.* **1999**, *192*, 587. (b) Horvath, I. T. *Acc. Chem. Res.* **1998**, *31*, 641.

Table 3. $M^{II}|M^{III}$ Oxidation Potentials of Arylated Ferrocenes and Cobaltocenes[a]

	$E_{1/2}$, mV			$E_{1/2}$, mV		
ferrocenes[b]	vs Cp_2Fe	vs SCE[c]	cobaltocenes[d]	vs Cp_2Co	vs SCE[e]	vs NHE[f]
Cp_2Fe[c]		410	Cp_2Co[e]		−910	−670
$[(C_6F_5)C_5H_4]_2Fe$ (**9**)[g]	348(5)	760	$[(C_6F_5)C_5H_4]_2Co$ (**13**)	400(5)	−510	−270
$[1,3\text{-}(C_6F_5)_2C_5H_3)_2Fe$ (**10**)[g]	680(5)	1090	$[1,3\text{-}(C_6F_5)_2C_5H_3)_2Co$ (**14**)	760(20)	−150	+90
$[1,2,4\text{-}(C_6F_5)_3C_5H_2]_2Fe$ (**11**)	940(10)	1350				
$[1,2,3\text{-}(C_6F_5)_3C_5H_2]_2Fe$ (**12**)	951(10)	1360				

[a] Experimental errors in parentheses are average deviations from the mean over at least two experiments. Complexes $[1,2,4\text{-}(C_6F_5)_3C_5H_2]_2Co$ (**15**) and $[1,2,3\text{-}(C_6F_5)_3C_5H_2]_2Co$ (**16**) were not sufficiently soluble for voltammetric analysis. [b] Dichloromethane solvent, 0.10 M TBAH electrolyte. [c] The potential of $Cp_2Fe|Cp_2Fe^+$ vs SCE was reported in ref 48a. The values in this column are approximations intended for comparison to the cobaltocene data and were obtained by adding 410 mV to the potentials obtained vs $Cp_2Fe|Cp_2Fe^+$ in dichloromethane. [d] Acetonitrile solvent, 0.10 M TBAH electrolyte. [e] The potential of $Cp_2Co|Cp_2Co^+$ vs SCE in acetonitrile was reported in ref 48b. The values in this column were obtained by subtracting 910 mV from the potentials obtained vs $Cp_2Co|Cp_2Co^+$ in acetonitrile. [f] The values in this column were obtained by adding 240 mV to the potentials obtained vs SCE. See ref 21. [g] Data from ref 13.

1). The diarylated complex **13** and the tetraarylated complex **14** are dark blue, while the hexaarylated complexes **15** and **16** are purple. The NMR spectra of **13**−**16** vary widely in their utility. Because these are paramagnetic compounds, extensive broadening and shifting of the resonances is expected. For example, the diarylated cobaltocene **13** showed two broad signals in the ^1H NMR spectrum (+29 and −45 ppm), but we could not identify any signals in the ^{19}F NMR spectrum. The tetraarylated cobaltocene **14** was the most recalcitrant, providing neither ^1H or ^{19}F NMR spectra that we could interpret, even when analyzing a concentrated sample. However, the hexaarylated cobaltocenes **15** and **16** provided satisfactory ^1H NMR spectra (one broad signal for each compound at 25 °C) and surprisingly sharp, well-resolved ^{19}F NMR spectra. The ^1H NMR spectra were most useful in confirming the *absence* of significant diamagnetic impurities such as hydrolyzed ligands or residual solvent in the purified complexes. Elemental microanalysis ultimately confirmed the composition and purity of these species.

Oxidation of Substituted Cobaltocenes. The relative stabilities of the cobaltocenes toward oxidation was particularly striking. Whereas Cp_2Co (formally a 19-electron complex) is relatively sensitive to air, the diarylated cobaltocene **13** is air-stable, and the tetraarylated **14** and hexaarylated cobaltocenes **15**, **16** are stable to air even in the presence of dilute aqueous hydrochloric acid. As the diarylated cobaltocene **13** is readily oxidized using air and dilute aqueous HCl (Scheme 1), we were able to isolate the corresponding diarylated cobaltocenium hexafluorophosphate **17** as an air-stable, yellow solid. In contrast, we observed the tetraarylated and hexaarylated cobaltocenium ions **18**−**20** only after dissolving the corresponding cobaltocenes **14**−**16** in concentrated sulfuric acid-d_2, whereupon the ^1H and ^{19}F NMR spectra showed spectra characteristic of the assigned diamagnetic $[(Ar_nCp)_2Co^{III}]^+$ ions (**18**, $n = 2$; **19** and **20**, $n = 3$), similar to those obtained for the isoelectronic ferrocenes **10**−**12**. The counterion associated with **18**−**20** was presumed to be either SO_4^{2-} or DSO_4^-.

Attempts to isolate the tetraarylated cobaltocenium ion **18** as the hexafluorophosphate failed; diluting the sulfuric acid solution of **18** led to the appearance of a blue-black solid having a ^{19}F NMR spectrum consistent with the cobaltocene **14**. This shows that water is a suitable reductant for $[(Ar_2Cp)_2Co^{III}]^+$. This behavior is reminiscent of classical coordination chemistry: $[(H_2O)_6\text{-}Co^{III}]^{3+}$ is unstable in the absence of stabilizing ligands such as NH_3 and is reduced by water to the corresponding Co^{II} ion.

These findings, which are corroborated by electrochemical measurements (see below), represent a "proof of concept" that C_6F_5 substituents can stabilize a 19-electron complex toward oxidation. We believe this stabilization arises from the electron-withdrawing tendency of the C_6F_5 groups, although crsytallographic characterization of a hexaarylated cobaltocene **16** suggests that fluorine atoms in *ortho* positions of the C_6F_5 groups may surround the Co atom and protect it from an approaching oxidant molecule. We are currently exploring the use of C_6F_5 groups to stabilize other "low oxidation state" organometallics metal species including zirconocene(II) species and 19-electron carbonylate anions.

Synthesis of Pentafluorophenyl-Substituted Mn and Re Piano Stool Complexes. Substitution reactions of either $Re(CO)_5Br$ or $Mn(CO)_5Br$ with arylated cyclopentadienylsodium ligands (Scheme 1) afforded the corresponding "piano stool" tricarbonyl complexes as yellow to orange (M = Mn, **21**−**24**) or colorless to tan (M = Re, **25**−**28**) solids. The infrared spectra of these complexes exhibit the expected two bands in alkane solution corresponding to A_1 and E symmetry-adapted internal coordinates for carbonyl-stretching deformations. The E bands are split in some cases as a result of perturbed C_{3v} symmetry.

The synthetic yields of substituted ferrocenes, cobaltocenes, and piano stool complexes reported here are low to moderate. Often, hydrolyzed ligands **1**−**4** were recovered during the workup and isolation of the desired complexes, suggesting either incomplete substitution reactions with the metal-containing precursors or hydrolysis of the ligands by adventitious moisture. The latter is a common problem with reactions carried out on a small scale, although we were careful to exclude moisture from our reactions as much as possible.

Physicochemical Evaluation of Electronic Substituent Effects. The hexaarylated ferrocenes **11** and **12** as well as the diarylated and tetraarylated cobaltocenes **13** and **14** were analyzed by solution voltammetry. The reversibility of the $Fe^{III}|Fe^{II}$ and $Co^{III}|Co^{II}$ couples was established using cyclic voltammograms (CVs), while the potential relative to internal $Fc^+|Fc$ (for **9**−**12**) and to internal $Cp_2Co^+|Cp_2Co$ (for **13** and **14**) was determined by square wave voltammetry. The potential data for these complexes (Table 3) reveal the expected monotonic and roughly linear increase in $E_{1/2}$ (Figure 1) with increasing ancillary arylation. The hexaarylated

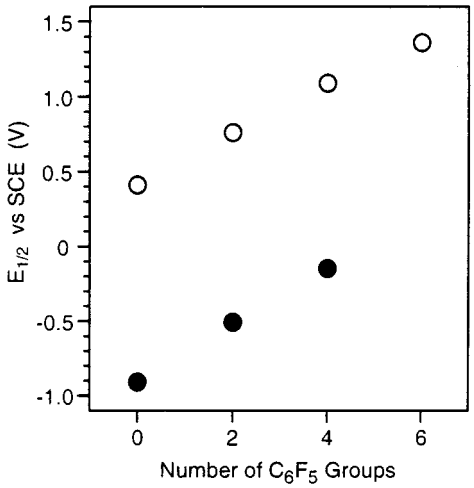

Figure 1. Plot of electrochemical potentials for ferrocenes (○) and cobaltocenes (●) as a function of the number of C_6F_5 substituents. Data were taken from Table 3.

Table 4. Carbonyl Stretching Wavenumbers of Piano Stool Complexes (Ar_nCp)M(CO)$_3$ (n = 0−3, M = Mn, Re, Ar = C_6F_5)

		wavenumbers (cm^{-1})[a]	
entry	complex	ν_{CO} (A)	ν_{CO} (E)
1.	$CpMn(CO)_3$ [b]	2028	1944
2.	$(ArCp)Mn(CO)_3$ (**21**)	2032	1954
3.	$(1,3\text{-}Ar_2Cp)Mn(CO)_3$ (**22**)	2035	1966, 1960
4.	$(1,2,4\text{-}Ar_3Cp)Mn(CO)_3$ (**23**)	2040	1973, 1965
5.	$(1,2,3\text{-}Ar_3Cp)Mn(CO)_3$ (**24**)	2041	1975, 1963
6.	$CpRe(CO)_3$ [b]	2031	1939
7.	$(ArCp)Re(CO)_3$ (**25**)[c]	2034	1947
8.	$(1,3\text{-}Ar_2Cp)Re(CO)_3$ (**26**)[c]	2038	1953
9.	$(1,2,4\text{-}Ar_3Cp)Re(CO)_3$ (**27**)	2042	1963, 1957
10.	$(1,2,3\text{-}Ar_3Cp)Re(CO)_3$ (**28**)	2043	1965, 1954

[a] Recorded in octane or hexanes solvent. Reproducibility is within 1 cm^{-1}. [b] Values of 2030 and 1946 cm^{-1} for $CpMn(CO)_3$ and 2032 and 1940 for $CpRe(CO)_3$ were reported elsewhere.[49] We prepared these complexes again for direct comparison with our compounds. [c] Prior results from our laboratories.[13]

cobaltocenes **15** and **16** were insufficiently soluble for reliable voltammetric measurements. Using standard reference potentials,[21] we found that the oxidation potentials of **13** and **14** vs NHE (Table 3) lie on either side of 0 V, rationalizing the observed difference in reactivity toward dilute aqueous HCl.

A clearly linear trend (Table 4, Figure 2) is also observed in the infrared spectra of substituted CpM(CO)$_3$ complexes (M = Mn, Re). The linear trends in these infrared spectroscopic and electrochemical data demonstrate that effects of up to six C_6F_5 substituents do not approach an electronic "limit", but rather the electronic structure of the metallocene and piano stool frameworks adjust to the influence of the substituents over a wide range.

Crystal Structures of Arylated Cyclopentadienes 2 and 4. As described in the Experimental Section, we obtained two distinct crystalline polymorphs of **2a** (**2-i** and **2-ii**) serendipitously. Relevant crystal data are collected in Table 1, selected metric data are presented in Table 5, and thermal ellipsoid plots are shown in Figure 3. The molecular structures are nearly

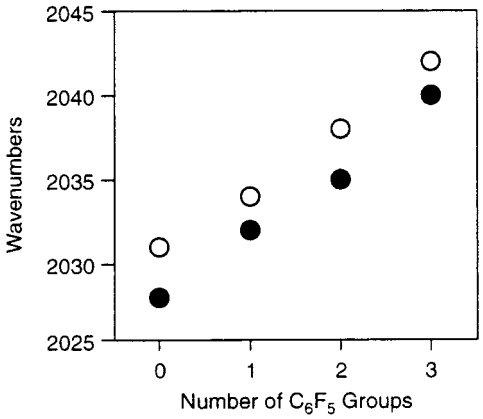

Figure 2. Plot of carbonyl stretching wavenumbers for $CpMn(CO)_3$ (●) and $CpRe(CO)_3$ (○) as a function of the number of C_6F_5 substituents. Wavenumber values have errors of ±1 cm^{-1}. Data were taken from Table 4.

Table 5. Selected Metric Data for 2a in Two Crystalline Polymorphs (i and ii)

bond distances (Å)			bond angles (deg)		
	2-i	**2-ii**		**2-i**	**2-ii**
C1−C2	1.481(2)	1.490(5)	C1−C2−C3	107.57(14)	107.7(3)
C2−C3	1.362(2)	1.338(5)	C2−C3−C4	109.79(14)	110.4(3)
C3−C4	1.443(3)	1.441(5)	C3−C4−C5	109.14(15)	109.6(3)
C4−C5	1.375(2)	1.356(4)	C4−C5−C1	107.67(14)	107.4(3)
C5−C1	1.471(2)	1.489(5)	C5−C1−C2	105.82(13)	105.0(3)
C2−C6	1.462(2)	1.471(4)	C1−C2−C6	124.56(13)	123.7(3)
C5−C12	1.467(2)	1.461(4)	C3−C2−C6	127.84(15)	128.6(3)
			C1−C5−C12	124.73(13)	124.6(3)
			C4−C5−C12	127.56(14)	128.0(3)

identical in the two polymorphs. The two double bonds of the five-membered core are significantly shorter than the three single bonds, and the C3−C4 single bond is also somewhat shortened, as expected for a conjugated diene. The nearly planar structures show Cp−C_6F_5 interplanar torsional angles (Table 6, entries 1−4) that are much smaller than those observed in fluorinated biphenyls such as 2,3,4,5,6-pentafluorobiphenyl (52.9%).[22] The corresponding angles observed for biphenyl (gas phase) are comparable,[23] whereas crystalline biphenyl is nearly planar.[24] Fluorinated biphenyls also typically exhibit arene stacking in the solid state.[22] Interestingly, neither **2-i** nor **2-ii** exhibits intermolecular arene stacking; however several intermolecular C−H···F−C interactions were identified (see below).

Although both polymorphs crystallized in monoclinic ($P2_1/c$) crystal systems, an interesting difference between the three-dimensional packing arrangements of **2-i** and **2-ii** is apparent in the relative orientations of face-to-face neighbors. In **2-i** (Figure 4(i)), neighboring molecular faces are related by simple translation along the crystallographic *b* axis, whereas in **2-ii** (Figure 4(ii)), molecular faces are instead related by the *c*-glide operation, leading to alternating orientations of the methylene carbon. Despite these differences, the dis-

(21) (a) Bard, A. J.; Faulkner, L. R. *Electrochemical Methods*; Wiley: New York, 1980; p 3. (b) Lu, S.; Strelets, V. V.; Ryan, M. F.; Pietro, W. J.; Lever, A. B. P. *Inorg. Chem.* **1996**, *35*, 1013.

(22) (a) Naae, D. G. *Acta Crystallogr.* **1979**, *B35*, 2765. (b) Brock, C. P.; Naae, D. G.; Goodhand, N.; Hamor, T. A. *Acta Crystallogr.* **1978**, *B34*, 3691.

(23) Almenningen, A.; Hartmann, A. O.; Seip, H. M. *Acta Chem. Scand.* **1968**, *22*, 1013.

(24) (a) Trotter, J. *Acta Crystallogr.* **1961**, *14*, 1135. (b) Charbonneau, G. P.; Delugeard, Y. *Acta Crystallogr.* **1976**, *B32*, 1420. (c) Charbonneau, G. P.; Delugeard, Y. *Acta Crystallogr.* **1977**, *B32*, 1586. (d) Gleason, W. B.; Britton, D. *Cryst. Struct. Commun.* **1976**, *5*, 483.

Table 6. Crystallographic C_6F_5−Cp Interplanar Conformational Angles

entry	compound	C_6F_5 group	Cp−C_6F_5 (deg)	entry	compound	C_6F_5 group	Cp−C_6F_5 (deg)
1.	**2-i**	C6−C11	13.0	13.	**16**	C11−C16	46.9
2.		C12−C17	15.4	14.		C21−C26	83.8
3.	**2-ii**	C6−C11	10.4	15.		C31−C36	49.4
4.		C12−C17	4.5	16.		C61−C66	52.6
5.	**4**[a]	C4−C7	57.0	17.		C71−C76	56.6
6.		C8−C13	54.8	18.		C81−C86	45.4
7.	**11**	C11−C16	39.6	19.	**23**·1/2C_6D_6	C9−C14	43.5
8.		C21−C26	77.0	20.		C15−C20	47.7
9.		C41−C46	30.7	21.		C21−C26	36.4
10.		C61−C66	36.7	22.	**26**	C9−C14	23.0
11.		C71−C76	75.2	23.		C15−C20	39.3
12.		C91−C96	27.3	24.	**27**	C9−C14	66.3
				25.		C15−C20	51.0
				26.		C21−C26	41.5

[a] Only two C_6F_5 groups in **4** are crystallographically unique.

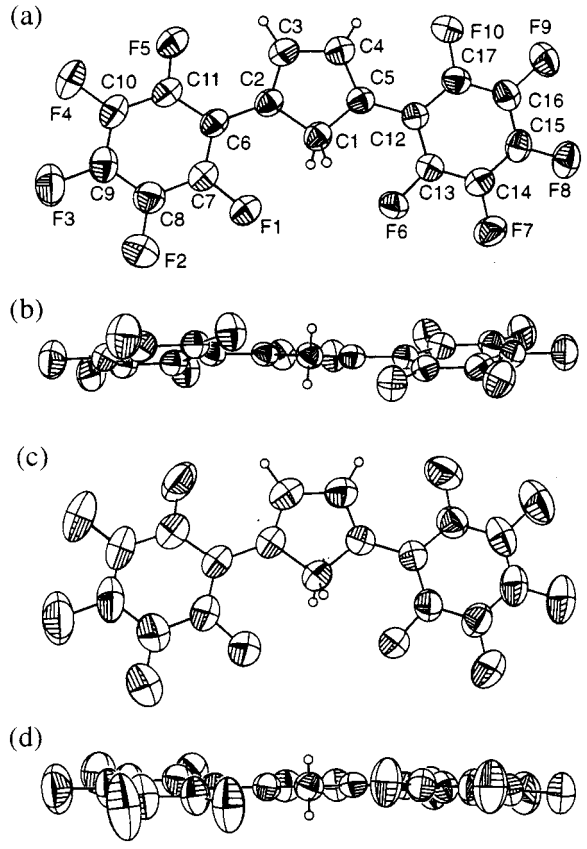

Figure 3. Thermal ellipsoid plots (50% probability) of the molecular structure of **2a** in two polymorphs. Numbering scheme is identical for both. (a) and (b) are **2-i**. (c) and (d) are **2-ii**.

tance between molecular least-squares planes for the two polymorphs was nearly identical (3.60 Å for **2-i** and 3.56 Å for **2-ii**), and the unit cell volumes are within 2% of one another.

We obtained crystals of **4** both to confirm our NMR-spectroscopic regiochemical assignment and to examine its molecular structure, particularly with regard to effects of the vicinal C_6F_5 substituents. Crystal data are presented in Table 1, metric data are shown in Table 7, and a diagram of the molecular structure is shown in Figure 5. The molecule exhibits crystallographic C_2 symmetry with the C1−C4 and C7−F3 bonds resting on the C_2 axis. Noteworthy is a 0.5:0.5 positional distortion that interchanges the methylene and methine carbon atoms (C3 and C3A). Packing diagrams reveal that the −C(3)H_2−C(3a)H− moiety fits snugly into a fluorinated "pocket" with crystallographically enforced C_2 symmetry. The Cp−C_6F_5 torsional angles (Table 6, entries 5 and 6) are much greater than the corresponding angles in **2a** (entries 1−4). Clearly, steric congestion among the three C_6F_5 substituents prevents the C_6F_5 groups from attaining more coplanar conformations relative to the C1−C5 ring. A similar difference is observed between biphenyl (torsion angle near 0°)[24] and 1,2-diphenylbenzene (torsion angles of 43° and 60°).[25]

Crystal Structures of Metallocenes. The molecular structure of the hexaarylated ferrocene **11** is shown in Figure 6. Examination of the metric data (Table 8) shows that the metallocene "core" of the complex exhibits nearly ideal pentahapticity within anticipated experimental errors. Both Cp rings are planar, with no carbon atom deviating more than 0.01 Å from its respective least-squares plane, and the interplanar angle between the Cp rings is 5.8(2)°.

In crystalline **11·4(C_6H_6)**, the six C_6F_5 substituents are held at varying torsional angles (27−77°) relative to the Cp ligands to which they are respectively attached (Table 6, entries 7−12). In previously reported C_6F_5-substituted ferrocenes *lacking* substituents vicinal to the C_6F_5 group, the C_6F_5 torsional angles are in the range 15.7−32.4°,[16] but the presence of a vicinal substituent (CH_2NMe_2 or $CH_2NMe_3^+$) increases the angle (40.7−54.8°).[35] Arene stacking is another striking feature of

(25) (a) Aikawa, S.; Maruyama, Y.; Ohashi, Y.; Sasada, Y. *Acta Crystallogr.* **1978**, *B34*, 2901. (b) Brown, G. M.; Levy, H. A. *Acta Crystallogr.* **1979**, *35*, 785.

(26) (a) Weck, M.; Dunn, A. R.; Matsumoto, K.; Coates, G. W.; Lobkovsky, E. B.; Grubbs, R. H. *Angew. Chem., Int. Ed.* **1999**, *38*, 2741. (b) Coates, G. W.; Dunn, A. R.; Henling, L. M.; Dougherty, D. A.; Grubbs, R. H. *Angew. Chem., Int. Ed. Engl.* **1997**, *36*, 248. (c) Williams, J. H. *Acc. Chem. Res.* **1993**, *26*, 593. (d) Lorenzo, S.; Lewis, G. R.; Dance, I. *New J. Chem.* **2000**, *24*, 295.

(27) (a) Basolo, F. *Pure Appl. Chem.* **1988**, *60*, 1193. (b) O'Connor, J. M.; Casey, C. P. *Chem. Rev.* **1987**, *87*, 307. (c) Marder, T. B.; Calabrese, J. C.; Roe, C. D.; Tulip, T. H. *Organometallics* **1987**, *6*, 2012. (d) Wescott, S. A.; Kakkar, A. K.; Stringer, G.; Taylor, N. J.; Marder, T. B. *J. Organomet. Chem.* **1990**, *394*, 777. (e) Faller, J. W.; Crabtree, R. H.; Habib, A. *Organometallics* **1985**, *4*, 929. (f) Carl, R. T.; Hughes, R. P.; Rheingold, A. L.; Marder, T. B.; Taylor, N. J. *Organometallics* **1988**, *7*, 1613.

(28) Nangia, A.; Desiraju G. R. *Top. Curr. Chem.* **1998**, *198*, 57.

(29) (a) Braga, D.; Grepioni, F. *Coord. Chem. Rev.* **1999**, *183*, 19. (b) Rivas, J. C. M.; Brammer, L. *Coord. Chem. Rev.* **1999**, *183*, 43.

(30) (a) Renak, M. L.; Bartholomew, G. P.; Wang, S. J.; Ricatto, P. J.; Lachicotte, R. J.; Bazan, G. C. *J. Am. Chem. Soc.* **1999**, *121*, 7787. (b) Row, T. N. G. *Coord. Chem. Rev.* **1999**, *183*, 81. (c) Evans, T. A.; Seddon, K. R. *Chem. Commun.* **1997**, 2023. (d) Williams, J. H.; Cockcroft, J. K.; Fitch, A. N. *Angew. Chem., Int. Ed. Engl.* **1992**, *31*, 1655.

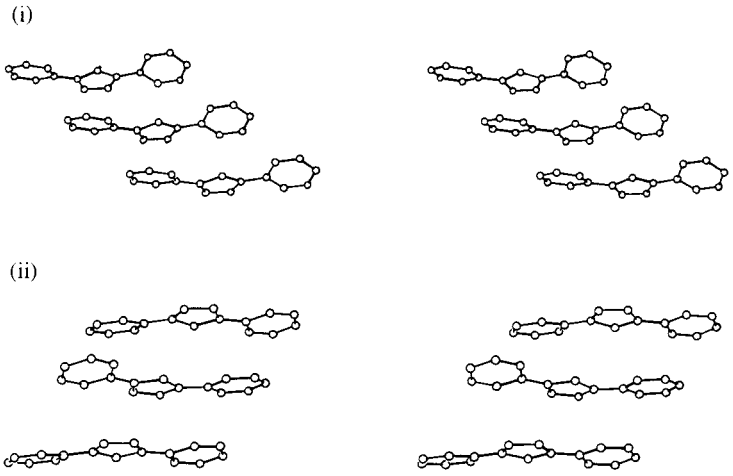

Figure 4. Partial crystallographic packing stereoviews of **2**. (i) Polymorph **2-i**. (ii) Polymorph **2-ii**. Hydrogen and fluorine atoms were omitted for clarity.

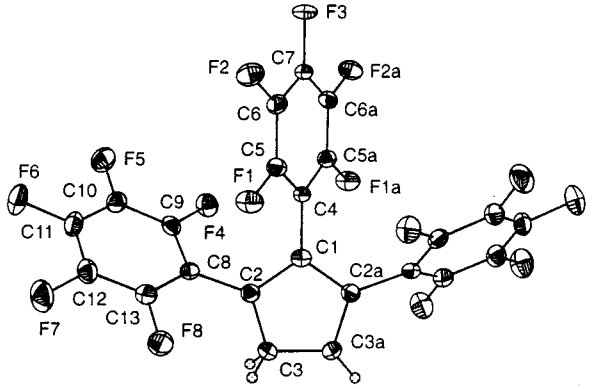

Figure 5. Thermal ellipsoid plot of **4** shown at 50% probability.

Table 7. Selected Metric Data for Crystalline 4

distances (Å)		bond angles (deg)	
C1−C2	1.4113(17)	C1−C2−C3	108.94(14)
C2−C3	1.420(3)	C2−C3−C3a	106.58(17)
C3−C3a	1.486(3)	C2a−C1−C2	108.95(11)
C1−C4	1.4761(15)	C2−C1−C4	125.52(8)
C2−C8	1.477(2)	C1−C2−C8	124.01(13)
		C3−C2−C8	127.05(15)

crystalline **11·4(C_6H_6)**. Each ligand has two C_6F_5 groups that are engaged in intramolecular C_6F_5−C_6F_5 stacking (Table 9, entries 1 and 2). Hughes and co-workers have rationalized this "slip-stacked" structural motif in crystalline **9** in terms of dipolar and quadrupolar charge distributions of the C_6F_5 groups.[16]

The striking tendency for nonfluorinated aryl groups and perfluoroaryl groups to engage in mutual stacking has also been the subject of recent experimental and theoretical investigation.[26] In **11·4(C_6H_6)**, both of the C_6F_5 groups that are *not* engaged in intramolecular

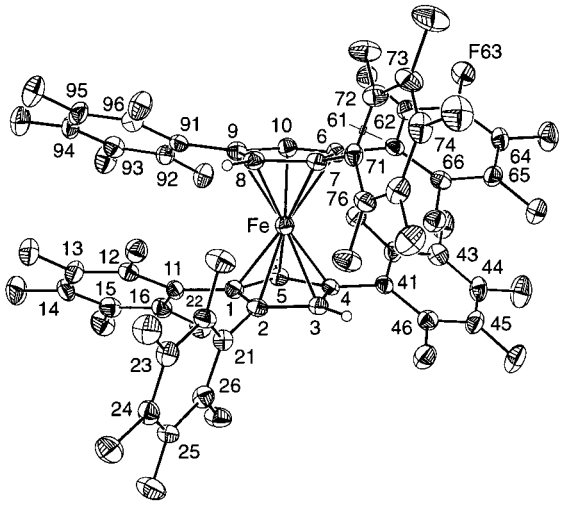

Figure 6. Thermal ellipsoid plot of **11·4(C_6H_6)**. Benzene solvate molecules were omitted for clarity. H and F atoms are numbered the same as the C atoms to which they are attached.

C_6F_5−C_6F_5 stacking are instead associated with benzene solvate molecules (entries 3 and 6). Two additional C_6F_5−C_6H_6 interactions (entries 4 and 5) arise from a benzene molecule "sandwiched" between two C_6F_5 groups of adjacent molecules. A packing diagram (Figure 7) shows this extended stacking motif. We were unable to grow crystals from C_6F_6 in order to examine the possibility of C_6F_5−C_6F_6 stacking in these complexes.

The fact that *all* of the C_6F_5 groups of **11** are engaged in some form of arene stacking suggests that this motif is a significant contributor to crystal packing. Metric data (Table 9) suggest less than idealized stacking interactions, as the least-squares planes are significantly nonparallel, and the centroid−centroid distances are relatively long, compared with those observed in crystalline **9** (entry 10). Arene stacking also influences the molecular structure (conformations) of **11**. Comparing the C_6F_5 torsion angles of the two "vicinal" C_6F_5 groups on each Cp ligand (Table 6), we observe that the C_6F_5 groups engaged in intramolecular C_6F_5−C_6F_5 stacking (entries 7 and 10) exhibit much smaller C_6F_5−Cp torsion angles than the C_6F_5 groups not so engaged (entries 8 and 11).

(31) Weck, M.; Dunn, A. R.; Matsumoto, K.; Coates, G. W.; Lobkovsky, E. B.; Grubbs, R. H. *Angew. Chem., Int. Ed.* **1999**, *38*, 2741.
(32) Thalladi, V. R.; Weiss, H.-C.; Bläser, D.; Boese, R.; Nangia, A.; Desiraju, G. R. *J. Am. Chem. Soc.* **1998**, *120*, 8702.
(33) This interaction was observed in bis(*N*-pentafluorophenyl)-tetraphenylcyclodisilazane benzene solvate. Two centroid−centroid distances are needed to describe this interaction, which does not appear at the crystallographic center. Claire, P.; Sowerby, D. B.; Haiduc, I. *J. Organomet. Chem.* **1986**, *310*, 161.
(34) (a) Gallivan, J. P.; Dougherty, D. A. *Org. Lett.* **1999**, *1*, 103. (b) Hernández-Trujillo, J.; Vela, A. *J. Phys. Chem.* **1996**, *100*, 6524.
(35) Deck, P. A.; Lane, M. J.; Montgomery, J. L.; Slebodnick, C.; Fronczek, F. R. *Organometallics* **2000**, *19*, 1013.

Table 8. Selected Bond Distances (Å) and Angles (deg) for the Metallocene Cores of 11·4(C_6H_6) (M = Fe) and 16 (M = Co)

	11·4(C_6H_6)	**16**		**11**·4(C_6H_6)	**16**
M−C1	2.071(2)	2.179(7)	M−C6	2.070(2)	2.168(7)
M−C2	2.071(2)	2.178(7)	M−C7	2.070(2)	2.143(7)
M−C3	2.061(2)	2.150(6)	M−C8	2.063(2)	2.129(7)
M−C4	2.067(2)	2.069(6)	M−C9	2.070(2)	2.070(6)
M−C5	2.039(2)	2.090(7)	M−C10	2.043(2)	2.097(7)
M−Cp(1)[a]	1.669(2)	1.760(7)	Cp(1)[a]−M−Cp(2)b	175.3(3)	179.4(8)
M−Cp(2)[b]	1.669(2)	1.743(7)			

[a] Cp(1) is the centroid of C1−C5. [b] Cp(2) is the centroid of C6−C10.

Table 9. Arene Stacking Interactions in Crystalline 11, 16, 23·1/2C_6D_6, and 9

entry	complex	aryl (1)	aryl (2)	OO (Å)[a]	OP (Å)[b]	α (deg)[c]
1.	**11**	C11−C16	C91−C96	3.78	3.23, 3.44	11
2.		C41−C46	C61−C66	3.72	3.32, 3.35	12
3.		C21−C26	C113−C118[d]	3.92	3.43, 3.64	9
4.		C41−C46	C107−C112[d]	4.02	3.45, 3.60	6
5.		C61−C66	C107−C112[d]	4.17	3.40, 3.83	14
6.		C71−C76	C101−C106[d]	3.79	3.78, 3.54	17
7.	**16**	C31−C36	C81−C86	4.20	3.51, 3.61	17
8.		C61−C66	C61−C66[e]	3.89	3.72	0
9.	**23**·1/2C_6D_6	C9−C14	C27−C29A[d]	3.57	3.41, 3.48	5
10.	**9**[f]	C_6F_5	C_6F_5	3.58	3.28, 3.32	5

[a] The distance between the two aryl C_6 centroids. [b] The distance between an aryl C_6 centroid and an aryl C_6 least-squares plane. If the two least-squares planes are not parallel, then two unique distances are calculated. [c] The angle between the two C_6 least-squares planes. [d] C_6D_6 solvate molecule. [e] Aryl (2) located on an adjacent molecule. [f] Parameters calculated from data provided in ref 16.

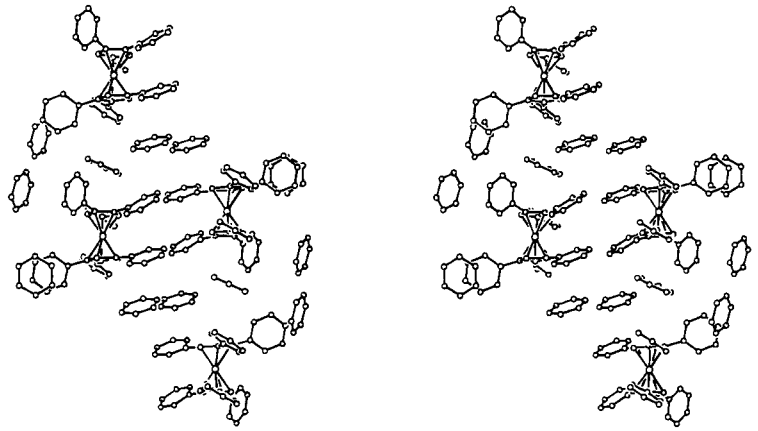

Figure 7. Partial packing stereoview of **11·4(C_6H_6)**, showing arene stacking motifs. H and F atoms omitted for clarity.

In the hexaarylated cobaltocene (**16**, Figure 8), the metallocene core is slightly distorted, as shown by some differences among the Co−C distances (Table 8), but not enough to suggest a "slipped" bonding mode.[27] The conformations adopted by five of the C_6F_5 substituents and their respective Cp ligands are described by torsion angles in the relatively narrow range of 45−57° (Table 6, entries 13 and 15−18), similar to the conformations observed in the corresponding cyclopentadiene (entries 5 and 6). The remaining C_6F_5 substituent (C21−C26) shows a nearly perpendicular Cp−C_6F_5 torsion angle of about 84° (entry 14). Six of the "ortho" F atoms (F16, F26, F32, F62, F72, and F82) encircle the cobalt atom with Co−F distances ranging from 3.40 to 3.64 Å (Figure 9). Such a "belt" of fluorine atoms may partly account for the astonishing stability of 19-electron complexes such as **16** toward air and dilute aqueous acids.

Crystalline **16** exhibits two interesting arene-stacking motifs (Table 9, entries 7 and 8), one intramolecular and one intermolecular. According to an empirical guideline that we established earlier,[35] the C_6F_5−C_6F_5 stacking interactions in crystalline **11** and **16** do not exhibit

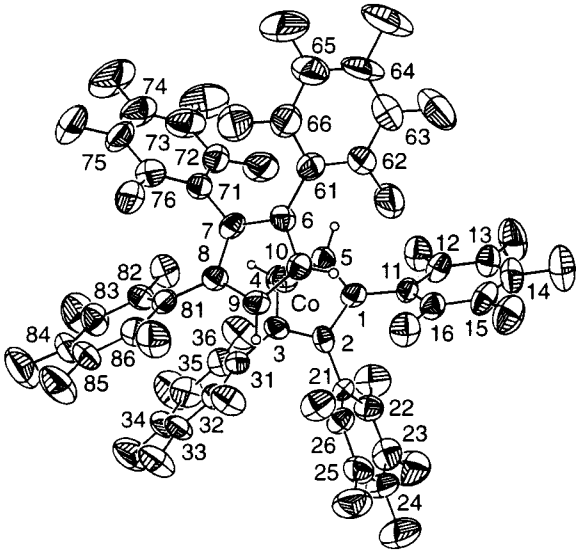

Figure 8. Thermal ellipsoid plot of **16** shown at 50% probability. H and F atoms are numbered the same as the C atoms to which they are attached.

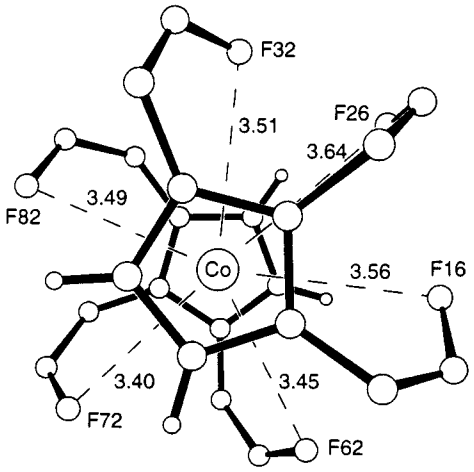

Figure 9. Partial molecular structure diagram for **16** showing a "belt" of aromatic fluorides circling the cobalt atom. Co···F distances are given in Å.

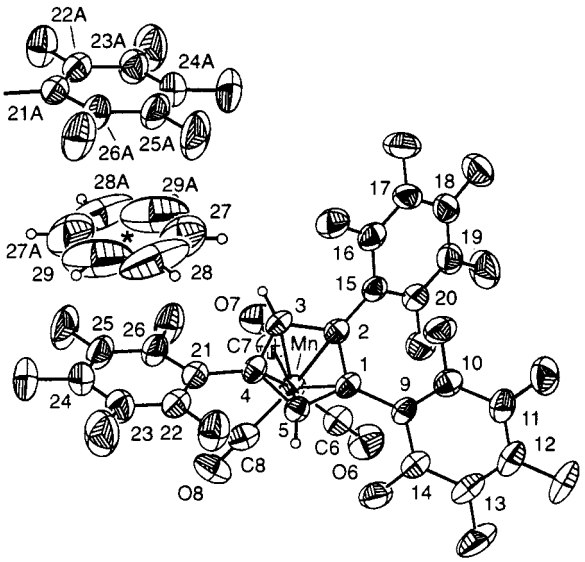

Figure 10. Thermal ellipsoid plot of **23·1/2(C$_6$D$_6$)** (50% probability) showing arene stacking of C_6D_6 solvate molecule between the C21−C26 and C21A−C26A pentafluorophenyl groups. H, D, and F atoms are numbered the same as the C atoms to which they are attached.

the degree of predictability needed for "crystal engineering".[16,28−32]

Crystal Structures of Piano Stool Complexes. When the manganese tricarbonyl complex **23** was crystallized from C_6D_6, crystals of an adduct having the empirical formula **23·1/2C$_6$D$_6$** were obtained (Figure 10). Solvent-free crystal structures of the rhenium tricarbonyl complexes (**26** and **27**) are shown in Figures 11 and 12, respectively. Metric parameters of the CpM(CO)$_3$ cores of these three complexes (Table 10) indicate no significant structural distortions. The three M−Cp distances fall well within the ranges (1.75 < Mn−Cp < 1.80 Å, 1.94 < Re−Cp < 1.96 Å) anticipated from a search of the Cambridge Crystallographic Database for analogous compounds. Likewise, the M−C−O parameters are not unusual. The torsion angles adopted by the C_6F_5 groups in these structures vary between 23° and 66° (Table 6, entries 19−26). Not surprisingly, the vicinal C_6F_5 groups (entries 19, 20, 24, and 25) are less

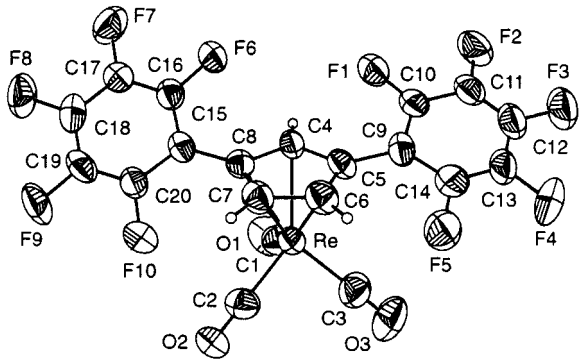

Figure 11. Thermal ellipsoid plot of **26** shown at 50% probability.

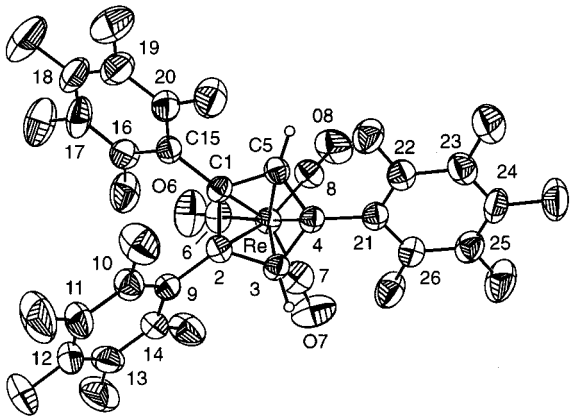

Figure 12. Thermal ellipsoid plot of **27** shown at 50% probability. H and F atoms are numbered the same as the C atoms to which they are attached.

Table 10. Selected Bond Distances (Å) and Bond Angles (deg) for the CpM(CO)$_3$ Cores of 23·1/2(C$_6$D$_6$) (M = Mn), 26 (M = Re), and 27 (M = Re)

	23·1/2(C$_6$D$_6$)	**26**	**27**
M−C$_{ring}$	2.174(3)	2.314(8)	2.309(6)
	2.164(3)	2.322(8)	2.331(6)
	2.130(3)	2.285(8)	2.299(5)
	2.149(3)	2.277(8)	2.302(6)
	2.139(4)	2.318(7)	2.298(6)
M−Cp[a]	1.780(4)	1.955(8)	1.968(6)
M−C$_{CO}$	1.795(4)	1.922(9)	1.904(7)
	1.790(4)	1.907(9)	1.915(9)
	1.790(4)	1.964(9)	1.902(6)
C−O	1.155(5)	1.136(12)	1.141(9)
	1.147(4)	1.158(11)	1.141(11)
	1.152(5)	1.087(13)	1.138(9)
M−C−O	178.5(4)	177.8(8)	179.5(6)
	177.3(3)	176.3(9)	177.3(6)
	176.5(3)	175.1(8)	177.0(6)

[a] Cp represents the centroid of the 5 Cp carbons.

coplanar compared with the "isolated" C_6F_5 groups (entries 21−23 and 26).

The C_6D_6 molecule of **23·1/2C$_6$D$_6$** rests on a crystallographic inversion center in a stacking arrangement between two C_6F_5 groups of **23**. This stacking feature (Table 9, entry 9) appears more ideal (shorter distances, rings closer to parallel) than that observed in **11·4(C$_6$H$_6$)**. Surprisingly, the interaction between C_6F_5 groups and solvate C_6H_6 (or C_6D_6) is not well documented in the Cambridge Crystallographic Database. The clearest, most compact example in the database is a "stack" analogous to that found in **23·1/2C$_6$D$_6$**, having slightly longer centroid−centroid distances of 3.713 and

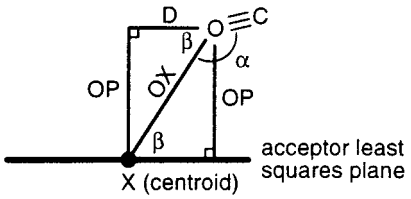

Figure 13. Definition of parameters used to characterize the intermolecular interactions of C_6F_5 groups with CO ligands.

Table 11. Intermolecular Donor−Acceptor Interactions of Carbonyl Ligands and Aromatic Rings in Crystalline Piano Stool Complexes 23·1/2C$_6$D$_6$, 26, and 27

entry	complex	donor	acceptor	OX (Å)[a]	OP (Å)[a]	α (deg)[a]	*D* (Å)[a]
1.	**23**·1/2C_6D_6	O6	C9−C14	3.12	3.10	126	0.33
2.	**23**·1/2C_6D_6	O7	C1−C5	3.15	3.11	126	0.51
3.	**26**	O1	C15−C20	3.06	2.93	171	0.86
4.	**27**	O6	C9−C14	3.65	3.13	170	1.88
5.	**27**	O7	C21−C26	3.36	2.86	133	1.76
6.	**27**	O8	C21−C26	3.18	3.06	150	0.85

[a] The parameters OX, OP, α, and *D* are defined in Figure 13.

3.719 Å, correspondingly longer centroid−plane distances of 3.614, 3.596, 3.704, and 3.709 Å, and interplanar angles of 3.4° and 5.3°.[33]

All three piano stool complexes **23·1/2C$_6$D$_6$**, **26**, and **27** exhibit directed, intermolecular interactions between the partially negatively charged oxygen terminae of the carbonyl ligands and the partially positively charged centroids of crystallographically neighboring C_6F_5 substituents. Metric parameters for these CO···C_6F_5 interactions are defined in Figure 13 and summarized in Table 11. These interactions are most striking in **27**, in which all three CO groups "contact" adjacent C_6F_5 groups (Figure 14). Of the five compounds in the Cambridge Crystallographic Database that exhibit OX distances less than 4.0 Å, only one shows an OX distance less than those reported here. The correlation ($r = 0.87$) of OX and D shown in Figure 15(a) suggests that donors approaching the *centroid* (decreasing OX) avoid van der Waals interactions with the fluorine atoms around the perimeter. However, poor correlation of OP with D shown in Figure 15(b) reveals that donors approaching the C_6F_5 plane (decreasing OP) do not tend to "zero in" on the central axis of the ring (decreasing D). Furthermore, neither **F** nor **G**, which we reported earlier, show any CO···C_6F_5 interactions.[14] Although this concept warrants further experimental (and theoretical) investigation, we must conclude for now that CO···C_6F_5 interactions are not useful design elements for crystal engineering. Well-organized interactions of perfluoroaromatic groups and lone pairs of electrons is documented.[34] Evidently the oxygen lone pairs of the CO ligands are much weaker donors than those previously studied. In the case of **23·1/2C$_6$D$_6$**, an additional C≡O···Cp(centroid) interaction is observed (Table 11, entry 2). This interaction is relatively common, and the metric details of the interaction observed for **23·1/2C$_6$D$_6$** are normal.

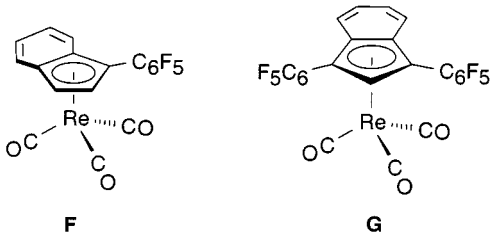

F **G**

C−H···F−C Interactions. Earlier reports from our laboratory[35] and elswhere[36] have attempted to establish specific parametric correlations as criteria for defining C−H···F−C as "hydrogen bonds." The sum of the van der Waals radii of hydrogen and fluorine is in the range 2.5−2.7 Å.[37] H···N and H···O hydrogen bonds generally exhibit distances that are *significantly shorter* than the sum of their respective van der Waals radii. Dunitz and Taylor suggested that a similar criterion should apply to H···F, which implies that an H···F distance less than 2.3 Å is necessary. In fact, 39 compounds having C−H···F−C contacts characterized by H···F distances less than 2.35 Å were found among 360 compounds containing sp^2-hybridized C−F bonds in the Cambridge Crystallographic Database.[38] However, interactions among organic C−F and C−H groups must often coexist with various other intermolecular packing motifs and compete with stronger donors and acceptors, which leads to a broad range of observed H···F distances and C−H···F angles.[32] Desiraju and Boese therefore advanced an alternative criterion of an inverse correlation between H···F distances and C−H···F angles based on a meticulous and exhaustive study of the fluorinated benzenes $C_6H_nF_{6-n}$.[32]

We recently extended their findings to fluoroarylated ferrocenes, in which C−H···F−C interactions are a persistent structural feature.[35] This extension was justified, because the C−H acidity of metallocenes is comparable with aromatic hydrocarbons and because the addition of the metal atom does not provide a competing hydrogen bond acceptor. We further classified as "purposeful" those C−H···F−C interactions that have H···F distances less than 3.0 Å and that lie within the inverse correlation demonstrated by Desiraju and Boese. Those having H···F distances less than 3.0 Å that diverge from the correlation were termed "diffuse". Importantly, our notion that "diffuse" and "purposeful"

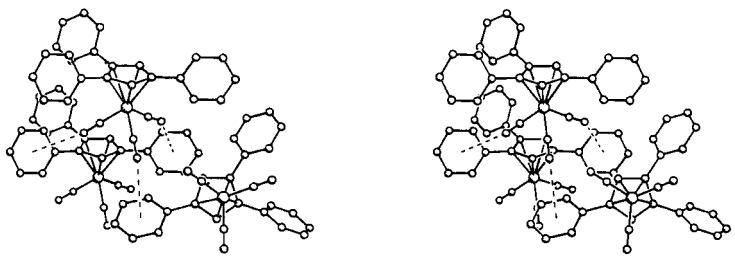

Figure 14. Partial packing stereoview of **27** showing CO···C_6F_5 interactions.

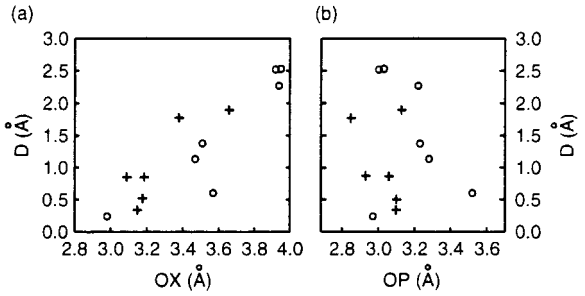

Figure 15. Correlations of metric parameters describing CO···C_6F_5 interactions. Parameters OX, OP, and D are defined in Figure 13. (+) Data from this work (Table 11); (○) data from the Cambridge Crystallographic Database.

C−H···F−C interactions can coexist in the same structure is not consistent with the Desiraju−Boese criterion of an inverse parametric correlation over all observed interactions. We assert that considerable allowance for "diffuse" interactions is not only justified but necessary, because the range of structural motifs and packing arrangements found in fluorinated benzenes (which are nearly isostructural) is not representative of all compounds in which one might want to look for C−H···F−C hydrogen bonds. In particular, other compounds often have extensive arrays of *intramolecular* C−H···F−C interactions, which tend to "saturate" hydrogen atoms, leading to much weaker intermolecular C−H···F−C interactions. The search for a more general understanding of C−H···F−C interactions is made much more difficult by these complications.

This section presents an analysis of the present crystal data in terms of these principles. We conducted an exhaustive search of all eight structures reported here for C−H···F−C interactions having H···F distances less than 3.0 Å and C−H···F angles greater than 100° (no angle restriction was enforced for intramolecular interactions). A complete table of all interactions is included in the Supporting Information (Tables S-65 and S-66). Figure 16 shows a scatterplot, in which the data reported by Desiraju and Boese are represented by small, unfilled circles. We added an elliptical region to encompass their data (only one point was excluded) and highlight the inverse correlation they proposed as a criterion for hydrogen bonding. The plot is dominated by 34 interactions (× symbols) observed among the C−F bonds and solvated benzene molecules in **11·4(C_6H_6)**. Although many of the new points in Figure 16 lie within the elliptical "correlation" region, the correlation between H···F distances and C−H···F angles for each individual compound is relatively poor. In fact, each of our compounds represented in the plot has a third to half of its respective points outside the shaded region. However, to pack into stable crystal structures, these irregularly shaped molecules cannot optimize all C−H···F−C interactions. We conclude that the strict requirement of a inverse distance−angle correlation is not necessarily appropriate for irregularly shaped molecules.

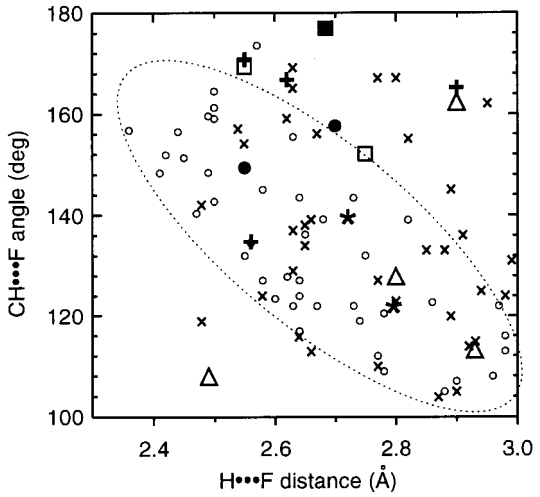

Figure 16. Scatterplot of C−H···F angles and H···F distances describing intermolecular C−H···F−C interactions in C_6F_5-substituted (cyclopentadienyl)metal complexes. (●) Data for **2-i**; (*) data for **2-ii**; (△) data for **4**; (×) data for **11**; (+) data for **16**; (□) data for **23**; (■) data for **27**; (○) data for fluorinated benzenes from ref 32.

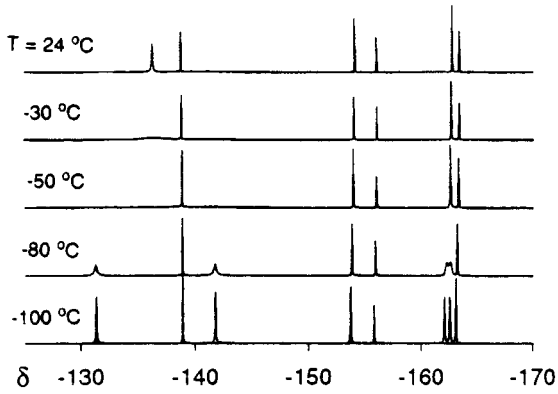

Figure 17. Stacked plot of ^{19}F NMR spectra of **27** obtained at several temperatures in THF-d_8 at 470 MHz.

Dynamic NMR Studies. Complexes **11**, **12**, and **27** were examined by variable-temperature ^{1}H and ^{19}F NMR spectroscopy in order to investigate their solution conformational dynamics. In the ^{19}F NMR spectrum of **27** (Figure 17), six signals were assigned to the *ortho* (−130 to −145 ppm), *meta* (−160 to −165 ppm), and *para* (−152 to −157) positions, respectively. At 25 °C, the presence of two signals (4:2 ratio) for the *ortho* fluorines signifies first that the two vicinal C_6F_5 groups are related by time-averaged molecular C_s symmetry and, second, that the endo and exo "edges" of the aryl groups are in the fast-exchange regime of the experiment. As temperature decreases, endo and exo *ortho* fluorines of the vicinal C_6F_5 groups decoalesce ($T_{coal} \approx$ −50 °C), whereas the "isolated" C_6F_5 group remains in fast exchange with respect to Cp−C_6F_5 rotation at −100 °C. Using eq 1 ($\Delta\nu$ = 4920 Hz at −100 °C), a first-order rate constant of exchange k_{coal} (at −50 °C) of 10 800 Hz is obtained for Cp−C_6F_5 rotation of the vicinal C_6F_5 groups. Temperature-dependent rate data obtained from line shape analysis[39] of the slow ($T \leq$ −60 °C) and fast exchange regimes (eq 2 and eq 3, respectively) enable

(36) (a) Grepioni, F.; Cojazzi, G.; Draper, S. M.; Scully, N.; Braga, D. *Organometallics* **1998**, *17*, 296. (b) Dunitz, J.; Taylor, R. *Chem. Eur. J.* **1997**, *3*, 89. (c) Plenio, H. *Chem. Rev.* **1997**, *97*, 3363.

(37) (a) Bondi, A. *J. Phys. Chem.* **1964**, *68*, 441. (b) Rowland, R. S.; Taylor, R. *J. Phys. Chem.* **1996**, *100*, 7384.

(38) Howard, J. A. K.; Hoy, V. J.; O'Hagan, D.; Smith, G. T. *Tetrahedron* **1996**, *52*, 12613.

(39) Hore, P. J. *Nuclear Magnetic Resonance*; Oxford Science: New York, 1995; pp 44−47.

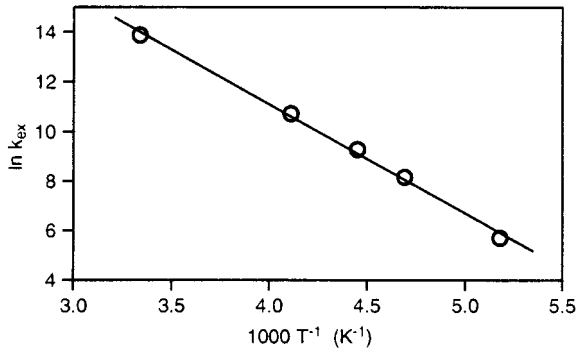

Figure 18. Arrhenius plot of C_6F_5−Cp rotational rate constants for **27**.

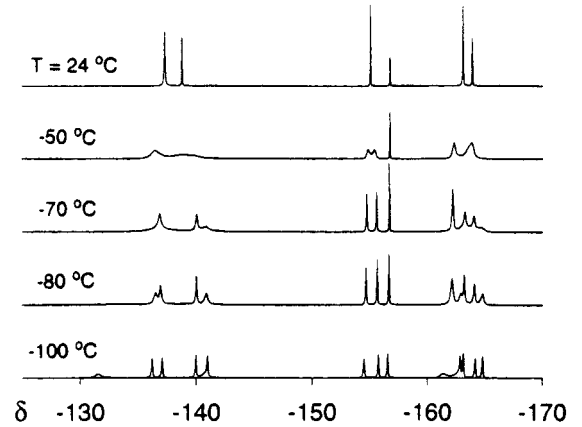

Figure 19. Stacked plot of ^{19}F NMR spectra of **11** obtained at several temperatures in THF-d_8 at 470 MHz.

the construction of an Arrhenius plot (Figure 18), from which we obtain an activation energy (E_a) of 9(1) kcal mol^{-1} for the rotation of adjacent C_6F_5 groups in **27**. The corresponding activation parameters, $\Delta H^{\ddagger} = 8(1)$ kcal mol^{-1} and $\Delta S^{\ddagger} = -2(5)$ cal mol^{-1} K^{-1}, obtained from an Eyring treatment agree qualitatively with a semiempirical (PM3) estimate ($\Delta H^{\ddagger} = 4.2$ kcal mol^{-1}) carried out on 1,2-bis(pentafluorophenyl)cyclopentadienyl anion.

$$k_{coal} = (\pi/\sqrt{2})\Delta\nu = 2.22\Delta\nu \quad (1)$$

$$k(T) = \pi[\text{fwhm}(T) - \text{fwhm(natural)}] \quad (2)$$

$$k(T) = \pi(\Delta\nu)^2/[\text{fwhm}(T) - \text{fwhm(natural)}] \quad (3)$$

Analysis of **11** by variable-temperature ^{19}F NMR spectroscopy reveals two dynamic processes. First, the Cp−C_6F_5 rotation of the "adjacent" C_6F_5 groups (as in **27**, discussed above) is evident from decoalescence of the signal at −137 ppm in the spectra obtained at $T \leq$ −50 °C (Figure 19). The second dynamic process involves relative rotation of the two Cp−Fe bonds[40] and is evident from the signal at −155 ppm (4 F), assigned to the *para* fluorines of the vicinal C_6F_5 substituents. At 25 °C, these four fluorines are interrelated by time-averaged C_{2h} symmetry, resulting in a single resonance. Decoalescence into two equally integrating resonances just above −50 °C shows that the ground state is represented by one of four canonical, diastereomeric structures (Figure 20, **b**−**e**), in which adjacent C_6F_5 groups on the same Cp ligand are inequivalent (loss of σ symmetry) while retaining C_2 relationships with counterparts on the opposite Cp ligand. Exchange of the two inequivalent C_6F_5 groups is a formal racemization process (Figure 20, **b** ⇄ **j**, **c** ⇄ **i**, **d** ⇄ **h**, or **e** ⇄ **g**), suggesting the use of a degenerate, two-site exchange model.

(40) (a) Okuda, J. *Top. Curr. Chem.* **1991**, *160*, 97. (b) Janiak, C.; Schumann, H. *Adv. Organomet. Chem.* **1991**, *33*, 291.

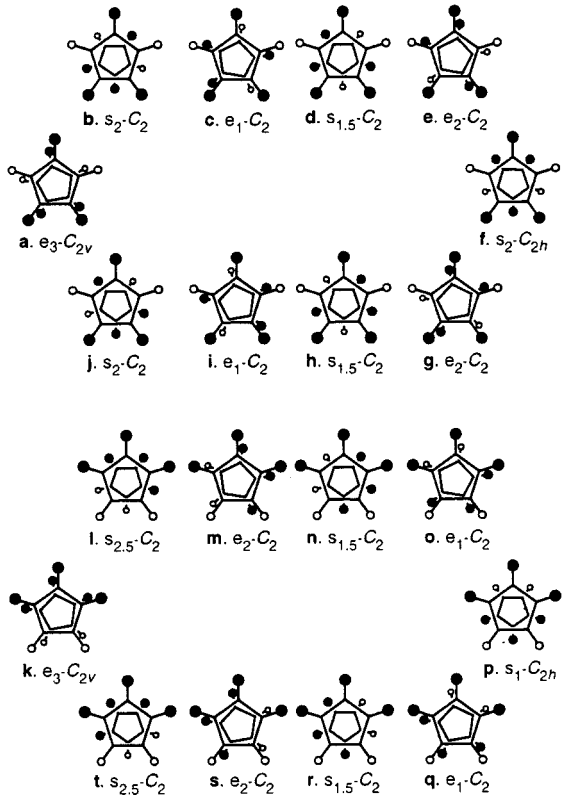

Figure 20. Conformational analyses of hexasubstituted metallocenes. Notation is described in the text.

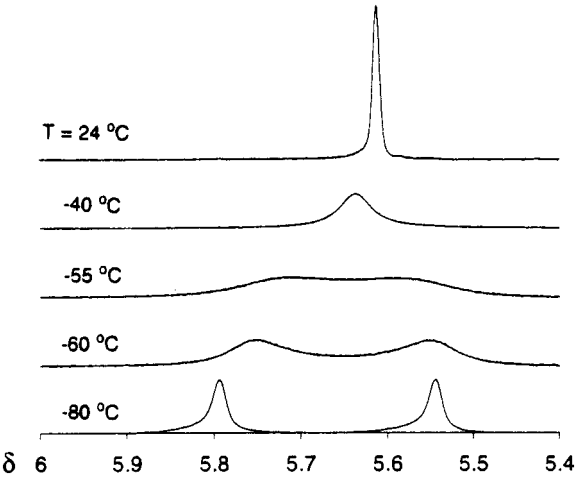

Figure 21. Stacked plot of ^1H NMR spectra of **11** obtained at several temperatures in THF-d_8 at 500 MHz.

Slowing the Cp−Cp rotation in **11** also leads to two signals in the ^1H NMR spectrum below about −50 °C (Figure 21). An Arrhenius plot (Figure 22) resulting from line shape analysis (eqs 2, 3) of the spectra shown in Figure 21 provides an activation energy (E_a) of 11(2) kcal mol^{-1} for this Cp−Cp rotation process with corresponding activation parameters ($\Delta H^{\ddagger} = 11(2)$ kcal mol^{-1} and $\Delta S^{\ddagger} = -2(5)$ cal mol^{-1} K^{-1}) obtained from an Eyring plot. Similar analysis of the ^{19}F NMR signals at −155

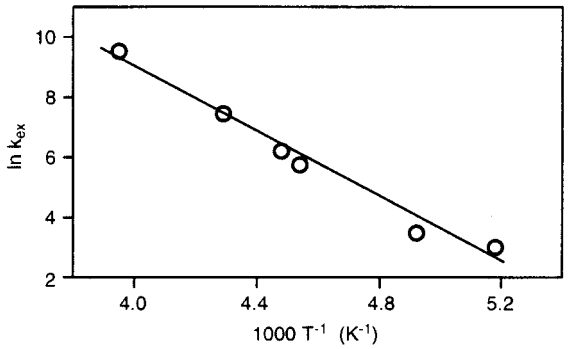

Figure 22. Arrhenius plot of Cp−Cp rotational rate constants for **11**.

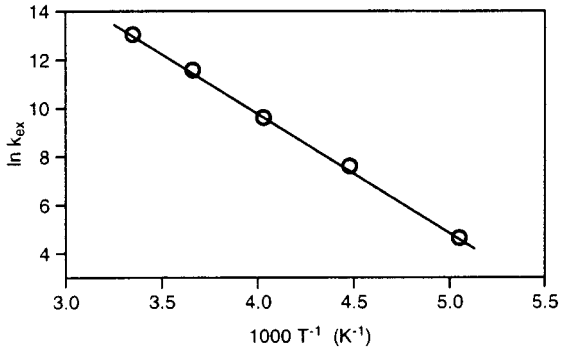

Figure 24. Arrhenius plot of Cp−C_6F_5 rotational rate constants for **12**.

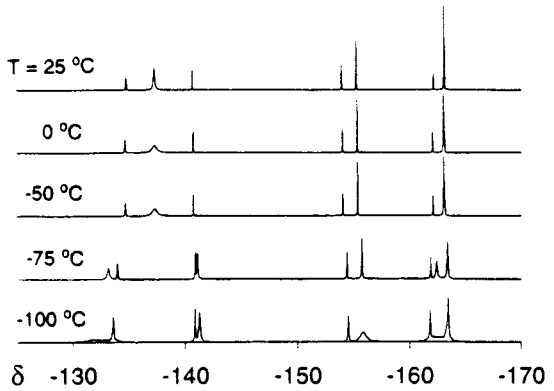

Figure 23. Stacked plot of ^{19}F NMR spectra of **12** obtained at several temperatures in THF-d_8 at 470 MHz.

ppm (Figure 19) corroborates this value. This activation energy[41] is comparable with those measured for [1,2,4-$(Me_3Si)_3C_5H_2]_2$Fe (11.0 kcal mol^{-1})[42] and [1,2,4-$(Me_3C)_3$-$C_5H_2]_2$Fe (15.3 kcal mol^{-1}),[43] but much larger than ferrocene itself (1.8−2.3 kcal mol^{-1}).[44]

Like **11**, the isomeric hexaarylated ferrocene **12** exhibits two dynamic processes in THF solution. First, rotation of the "outer" C_6F_5 groups about their respective C_6F_5−Cp bonds was evident from variable-temperature ^{19}F spectroscopy (Figure 23), and line shape analysis of the signals at −137 ppm led to an Arrhenius plot (Figure 24), which yielded an activation energy (E_a) of 10(1) kcal mol^{-1}. Eyring analysis of the same data gave $\Delta H^{\ddagger} = 9(1)$ kcal mol^{-1} and $\Delta S^{\ddagger} = -1(5)$ cal mol^{-1} K^{-1}. This value is within experimental error of the analogous process observed in **27**. The "middle" C_6F_5 groups of **12** do not rotate about their C_6F_5−Cp bonds at a rate that we could detect by ^{19}F NMR spectroscopy. No change in line shape of the diastereotopic *ortho* ^{19}F resonances was observed at 80 °C in 1,4-dioxane solution. The same "rotational locking" of the "middle" C_6F_5 group was also observed in all the other complexes prepared with this ligand (**16**, **20**, **24**, and **28**). These results contrast sharply with related studies in which $(Ph_4Cp)_2$Fe underwent rapid exchange of endo and exo phenyl protons on the "internal" phenyl groups at room temperature, with coalescence at −65 °C and $\Delta G^{\ddagger}_c = 9(1)$ kcal mol^{-1}.[45] Crude semiempirical modeling (PM3) predicted enthalpies of activation of 5.7 kcal mol^{-1} for 1,2,3-triphenylcyclopentadienyl anion and 13.5 kcal mol^{-1} for 1,2,3-tris(pentafluorophenyl)cyclopentadienyl anion. These findings illustrate the different steric effects of hydrogen and fluorine on aryl substituents.

The decoalescence of the signal assigned to the four *para* fluorines of the "outer" C_6F_5 groups of **12** (Figure 23, −100 °C spectrum, signal at −156 ppm) prohibits strict C_{2h} symmetry in the ground state and suggests a degenerate exchange process similar to that observed for **11**. Unfortunately, no estimate can be made of the activation barriers to Cp−Cp rotation in **12**. Although decoalescence occurs at a lower temperature in **12** than in **11**, the value of $\Delta\nu$ needed for eq 1 requires measurements in the slow-exchange spectral regime, which was inaccessible experimentally. The ^1H NMR spectra obtained at −100 °C show no line-broadening that we could attribute to chemical exchange, which is not surprising, as the spectral dispersion of ^1H NMR is much less than that of ^{19}F NMR.

Okuda proposed a simple but highly predictive strain-enthalpic quantifier to understand Cp−Cp rotational kinetics in substituted metallocenes (Figure 20).[42] Each eclipsing interaction (in eclipsed or "e" conformations) is assigned a value of +1 arbitrary enthalpy units, and each gauche interaction (in staggered or "s" conformations) is assigned a value of +0.5. Combining Okuda's conformational model (Figure 20) with the crystallographic data for **11** and **16**, and the NMR data for **11** and **12**, provides some insight into these dynamic processes while pointing to a potential limitation of Okuda's model for C_6F_5 substituents. An Okuda diagram for **11** (Figure 20) suggests that **c/i** (a pair of enantiomeric rotamers) should be the ground state of **11**, and indeed this is observed in [1,2,4-$(Me_3Si)_3C_5H_2]_2$-Fe,[42] whereas the crystallographic data presented above for **11** (Figure 6) argue for **e**/**g** instead. Okuda's model also predicts either **o**/**q** or **p** for the ground conformational state of **12**, but symmetry arguments (based on NMR data) presented above rule out **p**. Although we were unable to obtain crystals of **12**, the corresponding hexaarylated cobaltocene (**16**) adopts a structure about halfway between **o** and **p** (Figure 8).

(41) In some of the prior literature, E_a and $\Delta G^{\ddagger}$ appear to have been used interchangeably. We have cited only primary sources rather than review sources for the data presented here.

(42) Okuda, J.; Herdtweck, E. *Chem. Ber.* **1988**, *121*, 1899.
(43) Abel, E. W.; Long, N. J.; Orrell, K. G.; Osborne, A. G.; Šik, V. *J. Organomet. Chem.* **1991**, *403*, 195.
(44) (a) Holm, C. H.; Ibers, J. A. *J. Chem. Phys.* **1959**, *30*, 885. (b) Mulay, L. N.; Attalla, A. *J. Am. Chem. Soc.* **1963**, *85*, 702. (c) Makova, M. K.; Leonova, E. V.; Karimov, Y. S.; Kochetokova, N. S. *J. Organomet. Chem.* **1973**, *55*, 185.
(45) Castellani, M. P.; Wright, J. M.; Geib, S. J.; Rheingold, A. L.; Trogler, W. C. *Organometallics* **1986**, *3*, 1116.

According to Okuda's enthalpic descriptors, **11** and **12** should undergo facile exchange processes (**e** ⇄ **g** and **o** ⇄ **q**, respectively) with negligible enthalpic barriers. It is important to note that Okuda's model is derived from analysis of *tert*-butyl and trimethylsilyl substituents, which are much more isotropic with respect to Cp−R rotations than C_6F_5 groups. One might therefore expect that the anisotropic steric profile of C_6F_5 groups would facilitate Cp−Cp rotations, because transannular steric strain could be relieved considerably by adopting Cp−C_6F_5 torsional angles closer to 0° (coplanar rings). Indeed, detailed analysis of a three-dimensional model of **11** suggests that the exchange **e** ⇄ **g** requires synchronized (geared) rotations of the two pairs of stacked C_6F_5 groups. One member of each of these pairs (Figure 6) is a "vicinal" C_6F_5 group, for which the enthalpic barrier to Cp−C_6F_5 rotation is about 8 kcal mol^{-1} based on our analysis of the rhenium complex **27**. Two such rotations would account for more than the observed $\Delta H^{\ddagger}$ for Cp−Cp rotation in **11** (11 kcal mol^{-1}). In contrast, the exchange **o** ⇄ **q** proceeds with all C_6F_5 groups turning about their respective C_6F_5−Cp bonds through 90° torsion angles. Semiempirical (PM3) calculations on the 1,2-bis(pentafluorophenyl)cyclopentadienyl and 1,2,3-tris(pentafluorophenyl)cyclopentadienyl anions predict a much smaller barrier ($\Delta H^{\ddagger}$ < 2 kcal mol^{-1}) for this process. We would therefore expect **12** to undergo Cp−Cp rotation between the two enantiomeric ground-state rotamers to occur more rapidly. These findings suggest the need to couple Okuda's model for transannular steric strain with the conformational strain arising within a single ligand in order to arrive at a complete description of the fluxionality of perfluoroarylated metallocenes. The possibility of correlation among torsional degrees of freedom has been raised by others for related systems.[46]

The final inconsistency to address is the observation of **e**/**g** in crystalline **11** instead of the **c/i** conformation predicted by the Okuda diagram (Figure 20). Possibly, the positive enthalpy of an eclipsed interaction is reversed by attractive arene stacking forces. A distinct preference for arene stacking in 1,1′-bis(perfluoroaryl)-ferrocene complexes is already firmly established.[16,35] In that case, one might expect conformers **a** and **k** to be the preferred ground-state structures of **11** and **12**, respectively. Examination of three-dimensional models suggest that pairs of vicinal C_6F_5 groups cannot engage in ideal arene stacking, however, because of steric strain between *ortho* F atoms on vicinal C_6F_5 groups. This rationalizes the crystallographic observation of conformer **o** (a single pair of stacked C_6F_5 groups) instead of **m**/**s** (two stacking pairs) or **k** (three stacking pairs) in the hexaarylated cobaltocene (**16**). Of course, a crystal structure of **10** would address this hypothesis, but so far we have been unable to obtain these data. The most closely related complex that we have been able to characterize crystallographically is the methylated ferrocene (**H**), which indeed shows pairwise, intramolecular stacking of all four C_6F_5 groups.[47]

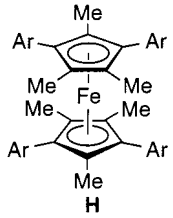

H

Conclusions. Up to three pentafluorophenyl (C_6F_5) substituents are readily attached to cyclopentadiene by nucleophilic aromatic substitution reactions of cyclopentadienyl anions with hexafluorobenzene. Cyclopentadienyl anions bearing one, two, or three C_6F_5 groups serve as ligands to form stable, well-characterized ferrocenes and cobaltocenes, as well as piano stool complexes of manganese and rhenium. The electron-withdrawing ability of the C_6F_5 substituents is evident from large shifts in the $E°$ of oxidation of substituted ferrocenes and cobaltocenes and in the carbonyl stretching wavenumbers of substituted Mn and Re piano stool complexes. The ability of C_6F_5 groups to stabilize 19-electron complexes is illustrated for cobaltocene; with four or more C_6F_5 substitutents, cobaltocene is stable to air in the presence of dilute hydrochloric acid. C_6F_5-substituted (cyclopentadienyl)metal complexes exhibit pervasive structural motifs: orderly arene stacking, close $C_6F_5\cdots O{\equiv}C$ contacts, and diffuse C−H···F−C interactions. Conformational dynamics in ferrocenes bearing multiple C_6F_5 substituents are described by a qualitative model in which transannular steric interactions governing Cp−Fe−Cp rotational barriers are synchronized (coupled) with Cp−C_6F_5 torsions, resulting in an overall enthalpic barrier to Cp−Fe−Cp that is similar to corresponding Me_3Si-substituted ferrocenes.

Acknowledgment. J. L. Montgomery, an undergraduate research participant, provided some of the electrochemical analyses of arylated cobaltocenes. We thank T. Glass for assistance with NMR analyses. Fruitful discussions with Professors R. P. Hughes (Dartmouth College), T. W. Hanks (Furman University), and J. R. Sowa (Seton Hall University), are gratefully acknowledged. This project was supported by the Petroleum Research Fund (30738-G) and the Virginia Tech Chemistry Department.

Supporting Information Available: Tables (S1−S64) of crystallographic data for **2-i**, **2-ii**, **4**, **11·4(C_6H_6)**, **16**, **23·1/2(C_6D_6)**, **26**, and **27**; tables of C−H···F−C interactions (S65, S66); two figures (S1, S2) showing semiempirical modeling results, and a detailed procedure for the preparation of **1**. This information is available free of charge on the Internet at http://pubs.acs.org.

OM000798V

(46) (a) Gupta, H. K.; Stradiotto, M.; Hughes, D. W.; McGlinchey, M. J. *J. Org. Chem.* **2000**, *65*, 3652. (b) Iwamura, H.; Mislow, K. *Acc. Chem. Res.* **1988**, *21*, 175.

(47) Unpublished results from our laboratories.

(48) (a) Robbins, J. L.; Edelstein, N.; Spencer, B.; Smart, J. C. *J. Am. Chem. Soc.* **1982**, *104*, 1882. (b) Koelle, U.; Khouzami, F. *Angew. Chem., Int. Ed. Engl.* **1980**, *19*, 640.

(49) (a) Benson, I. B.; Knox, S. A. R.; Stansfield, R. F. D.; Woodward, P. *J. Chem. Soc., Dalton Trans.* **1981**, 51. (b) Casey, C. P.; Rutter, E. W. *Inorg. Chem.* **1990**, *29*, 2333.